HIF-1 reduces myocardial ischaemia-reperfusion injury by targeting the mitochondria permeability transition pore

Sang-Ging Ong[1,2,5]; Won Hee Lee[2,5]; Louisa Theodorou[1]; Kazuki Kodo[2]; Shiang Y Lim[1]; Deepa H Shukla[3]; Thomas Briston[3]; Serafim Kiriakidis[4]; Margaret Ashcroft[3]; Sean M Davidson[1]; Patrick H Maxwell[3]; Derek M Yellon[1]; Derek J Hausenloy[1]

[1]The Hatter Cardiovascular Institute, University College London & Medical School, UK. [2]Department of Medicine, Division of Cardiology, Stanford University, Stanford, USA. [3]Centre for Cell Signalling and Molecular Genetics, University College London & Medical School, UK. [4]Kennedy Institute of Rheumatology, NDORMS, University of Oxford, UK.

[5]These authors contributed equally.

Address for Correspondence:

Derek J Hausenloy, MD, PhD

The Hatter Cardiovascular Institute,

University College London,

67 Chenies Mews,

London, WC1E 6HX,

United Kingdom.

Tel: +44 203 447 9888

Fax: +44 203 447 5095

Email: d.hausenloy@ucl.ac.uk

Total Word Count: 5722 words

Keywords: energy metabolism, hypoxia inducible factor (HIF), ischaemia, mitochondria, reperfusion

Nonstandard Abbreviations and Acronyms:

AAR	Area at risk
HIF-1α	Hypoxia-inducible factor-1 alpha
HKII	Hexokinase II
IHD	Ischaemic heart disease
IPC	Ischaemic preconditioning
IPC	Ischaemic preconditioning
IRI	Ischaemia-reperfusion injury
MPTP	Mitochondria permeability transition pore
OXPHOS	Oxidative phosphorylation
PDK1	Pyruvate dehydrogenase kinase
PHD	Prolyl hydroxylase
ROS	Reactive oxygen species
TMRE	Tetramethylrhodamine, ethyl ester
VHL	Von Hippel-Lindau tumor suppressor protein

1. Introduction

Ischaemic heart disease (IHD) is the leading cause of death globally, accounting for over a million deaths annually.[1] The effects of IHD are attributable to the detrimental effects of acute myocardial ischaemia-reperfusion injury (IRI) on the myocardium. Despite optimal therapy the morbidity and mortality in IHD patients remains significant, paving the way for the new treatment strategies for protecting the heart against acute IRI.

Various experimental studies have suggested that the stabilisation of hypoxia-inducible factor-1 (HIF-1) under normoxic conditions may confer tolerance against acute myocardial IRI.[2-7] However, the actual mechanism through which HIF-1 mediates its cardioprotective effect is unknown. Following a sustained episode of myocardial ischaemia, and in early reperfusion, the prevailing conditions of mitochondrial calcium and phosphate overload, oxidative stress, and relative ATP depletion, induce the opening of the mitochondrial permeability transition pore (MPTP), a critical event which results in cardiomyocyte death. Pharmacological inhibition of the MPTP at this time has been demonstrated in experimental studies[8-10] and one clinical study[11] to reduce MI size by 40-50%. Whether the stabilisation of HIF-1 protects the heart against acute IRI by inhibiting MPTP opening has not previously been investigated. In this study, we demonstrate for the first time that normoxic stabilisation of HIF-1 protects the heart against IRI by limiting MPTP opening through a metabolic switch, and that mitochondrial HKII is partially required for HIF-1 in maintaining mitochondrial integrity.

2. Methods

An extended version of the methods applied in this study is provided in the Supplementary material online.

2.1 Animals

Animals were treated in accordance with the Animals (Scientific Procedures) act 1986, published by the UK Home Office. All procedures were approved under Project license number PPL 70/6281 and 70/7140 ("Protection of the Ischaemic and Reperfused Myocardium").

Male Sprague-Dawley (SD) rats (350-400g) were obtained from the Biological Services Unit of University College London (United Kingdom). Rats were anesthetised by intraperitoneal injection of pentobarbital (50 mg/kg). Hearts were then excised and used for ex vivo Langendorff-perfusion or isolation of cardiomyocytes. Rats were administered by oral gavage, the PHD inhibitor, GSK360A (30 mg/kg), or DMSO 4 hours prior to myocardial infarction, in order to investigate the effects of *in vivo* stabilisation of HIF-1α on cardioprotection. To dislodge mitochondrial HKII, hearts were perfused with HKII-dissociating peptide or control peptide during the last 20 minutes of stabilisation at 200 nM.

$VHL^{flox/flox}$ mice (The Jackson Laboratory) were crossed with mice containing tamoxifen-inducible cardiac-specific α-Myosin heavy chain promoter driven MerCreMer transgene to generate $VHL^{fl/fl}$; α-MHC-Cre mice ($VHL^{fl/fl}$). Mice were aneasthetised by intraperitoneal injection with a combination of ketamine, xylazine, and atropine (0.01 mL/g, final concentrations of ketamine, xylazine, and atropine 10 mg/mL, 2 mg/mL, and 0.06 mg/mL, respectively) before being subjected to in vivo MI or harvesting of hearts for cardiomyocytes isolation.[12]

2.2 In vitro experiments

HL-1 cells were cultured as previously described.[13] Where indicated, cells were treated with either DMSO or GSK360A. siRNA experiments were performed 24 hours prior to DMSO or GSK360A treatment. mRNA and protein expression were analysed by real-time PCR and Western blot, respectively. Detailed proteomic analysis is described in Supplementary material online. Oxygen consumption was monitored using the fluorescent oxygen probe MitoXpress-Xtra-HS according to manufacturer's instructions. Fluorescence microscopy was performed to determine resting mitochondrial membrane potential (TMRE), basal mitochondrial ROS (MitoTracker Red CM-H_2XRos), mitochondrial superoxide (MitoSox

Red) and MPTP opening (Image-IT LIVE Mitochondrial Transition Pore Assay Kit) respectively. Intracellular lactate and glycogen levels were determined using kits from Biovision Inc. Staining of glycogen was performed using a Periodic acid-Schiff staining from Sigma-Aldrich according to manufacturer's instructions. *In vitro* IRI was performed by subjecting cells to ischemia followed by reperfusion. Cell death was determined by propidium iodide staining. Dislodgement of mitochondrial HKII was induced by treating cells with HKII-peptide (5 μM). All procedures were performed as previously described.[12, 14]

2.3 Statistical Analysis

The data shown are presented as the mean ± standard error of three or more independent experiments. Differences are considered statistically significant at $P<0.05$, assessed using the Student's *t* test (for paired samples) or the ANOVA test (for more than two groups) followed by post-hoc analysis using Tukey's test

3. Results

3.1 GSK360A treatment of HL-1 cells stabilised HIF-1

Treatment of the HL-1 cardiac cell line under normoxic conditions with a novel prolyl hydroxylase (PHD) inhibitor, GSK360A (25 or 50 μM) for varying time durations led to increased gene expression of several candidate HIF-1 target genes (*Figure 1A*). Subsequent experiments were performed on HL-1 cells treated for 8 hours with 50 μM of GSK360A as this dosing regimen promoted an increase in the glycolytic-related genes PDK1 and HKII. Immunoblotting of whole cell lysate further confirmed an increase in HIF-1α protein levels, and this corresponded with an increase in HKII in the purified mitochondrial fraction (*Figure 1B*). Importantly, treatment of HL-1 cells with GSK360A failed to induce activation of HIF-1 target genes except HO-1, when cells were pretreated with siRNA targeting HIF-1α (*Figure 1C*, Supplementary material online, *Figure S1*). These results indicate that treatment of HL-1

cells with GSK360A stabilised HIF-1α under normoxic conditions resulting in the transcription of downstream genes.

3.2 GSK360A treatment of HL-1 cells promoted aerobic glycolysis

In order to explore the molecular pathways regulated by normoxic HIF-1 stabilisation, we subjected whole cell extracts harvested from cells treated with either DMSO or GSK360A to relative quantitative proteomic analysis (*Figure 2A*). Using a fold change cut-off of $\geq$ 2, 49 proteins were found to be down-regulated by GSK360A treatment whereas 81 proteins were shown to be up-regulated (Supplementary material online, *Table I* and *Table II*). Gene ontology analysis using the PantherDB database revealed an enrichment in the percentage of proteins involved in metabolic processes and the generation of precursor metabolites and energy (*Figure 2B*), which is in accordance with previous studies implicating metabolic reprogramming away from oxidative phosphorylation (OXPHOS) towards aerobic glycolysis with HIF-1 stabilisation.[15, 16] Accordingly, we observed lower oxygen utilisation in HL-1 cells treated with GSK360A compared to DMSO-treated cells when measured using a fluorescent oxygen probe (representative image of a single experiment shown in *Figure 2C*). Relative oxygen consumption of GSK360A-treated cells was also significantly lower when measured at different time intervals (*Figure 2D and 2E*). This metabolic switch was dependent on HIF-1, because HL-1 cells depleted of HIF-1 failed to demonstrate reduced oxygen consumption following GSK360A treatment (*Figure 2D and 2E*). The role of HKII as a downstream effector of HIF-1 mediated metabolic switch was also confirmed by knockdown of HKII, which partially prevented HL-1 cells from decreasing oxygen consumption despite GSK360A treatment (*Figure 2D and 2E,* Supplementary material online, *Figure S2*).

To further characterise the metabolic switch from OXPHOS to aerobic glycolysis mediated by normoxic HIF-1 stabilisation, we measured mitochondrial membrane potential ($\Delta\psi_m$) and mitochondrial reactive oxygen species (ROS) production under basal conditions. Cells treated with GSK360A had a significantly lower $\Delta\psi_m$ as measured by reduced TMRE fluorescence, compared with DMSO-treated cells

alone (*Figure 3A*). As mitochondrial ROS are generated during OXPHOS, we also investigated whether GSK360A treatment would decrease mitochondrial ROS levels. We examined mitochondrial ROS in DMSO-treated and GSK360A-treated cells using MTR CM-H_2XRos, a mitochondrial specific dye that fluoresces when oxidized by ROS. Under basal conditions, GSK360A-treated cells showed significantly lower levels of mitochondrial ROS compared with vehicle-treated cells (*Figure 3B*). Consistent with the decrease in OXPHOS, GSK360A also decreased the expression of antioxidant genes (*Figure 3C*) and conversely led to an increase in intracellular lactate levels (*Figure 3D*). Previous studies have reported an increase in glycogen levels when cells were exposed to hypoxia or hypoxia-mimetics.[17] However, HL-1 cells treated with GSK360A for 8 hours had comparable intracellular glycogen compared to DMSO-treated cells indicating that short-term stabilisation of HIF-1α in our study does not lead to accumulation of glycogen (*Figure 3E*).

3.3 GSK360A treatment protected HL-1 cells against acute IRI – a role for HKII

We next investigated whether HIF-1-induced reprogramming of basal metabolism is relevant for protection against acute IRI and whether this effect is mediated by the HIF-1 downstream target gene, HKII. HL-1 cells were pre-treated with either DMSO or GSK360A before being subjected to *in vitro* simulated IRI. Cell death was then determined by propidium iodide (PI) exclusion and mitochondrial HKII levels were measured by immunoblotting. As evidenced in *Figure 4A*, cells treated with GSK360A had significantly lower cell death compared to DMSO-treated cells and this was associated with increased mitochondrial HKII levels (*Figure 4B*). To investigate the role of HIF-1 and HKII in mediating this protective effect, cells treated with siRNA against HIF-1 or HKII were subjected to a similar protocol. Indeed, knockdown of HIF-1 completely abolished the protective effects of GSK360A leading to increased cell death compared to DMSO-treated cells while knockdown of HKII abolished the protective effects of GSK360A (*Figure 4A*). Immunoblotting of HKII revealed that knockdown of either HIF-1 or

HKII resulted in decreased HKII levels in isolated mitochondrial fraction, demonstrating the protective effects of HIF-1 against IRI were partially dependent on mitochondrial HKII (*Figure 4B*).

To further investigate the mechanism by which IRI is attenuated by normoxic HIF-1 stabilisation, we evaluated mitochondrial function in HL-1 cells during reperfusion focusing on oxidative stress and MPTP opening, both of which are important mediators of cell death at this time and have been reported to be modulated by mitochondrial HKII. Consistent with lower cell death, GSK360A-treated cells exhibited less mitochondrial oxidative stress after IRI as indicated by reduced fluorescence of MitoSOX Red which fluoresces upon oxidation by mitochondrial superoxide (*Figure 4C*). This was accompanied by inhibited MPTP opening as indicated by improved retention of mitochondrial-entrapped calcein-AM following reperfusion (*Figure 4D*). In this assay, MPTP opening during reperfusion allows the redistribution of mitochondrial localised calcein to the cytosol where its fluorescence is quenched. In contrast, siRNA targeting HIF-1 resulted in higher oxidative stress and increased MPTP opening in cells treated with GSK360A demonstrating its dependence on HIF-1 in mediating cardioprotection against IRI (*Figure 4C and 4D*). The role of HKII in HIF-1 mediated cardioprotection was also demonstrated by experiments in which cells pre-treated with a siRNA targeting HKII followed by GSK360A treatment failed to limit production of oxidative stress and prevent MPTP opening following IRI (*Figure 4C and 4D*).

3.4 GSK360A treatment protected the rat heart against acute IRI – a role for HKII

Having demonstrated in HL-1 cells the importance of the HIF-1-HKII axis in mediating resistance against IRI by inhibiting MPTP opening, we investigated this protective pathway in Langendorff-perfused adult rat hearts rat hearts subjected to acute IRI. *In vivo* pre-treatment of rats with GSK360A, administered 4 hours earlier by oral gavage resulted in a significant increase in myocardial HIF-1α stabilisation as assessed by immunostaining (*Figure 5A*), and qPCR of HIF-1 target genes (Supplementary material online, *Figure S3*). Although there was no difference in area at risk (AAR) in these excised hearts compared to DMSO-treated hearts following regional LAD occlusion and reperfusion (*Figure 5B*),

GSK360A treatment significantly reduced myocardial infarct size compared to control animals (*Figure 5C*, Supplementary material online, *Figure S4*). To investigate the functional importance of mitochondria-HKII association underlying HIF-1-induced cardioprotection, we used a synthetic peptide that contains a cellular uptake motif and the mitochondrial binding motif of HKII that has been shown to acutely dislodge HKII from mitochondria.[18, 19] Isolated hearts from DMSO or GSK360A-treated rats were perfused with this HKII-peptide during the initial stabilisation period, before being subjected to regional LAD occlusion. Treatment with this HKII peptide treatment decreased the association of HKII with mitochondria following reperfusion (*Figure 5D*) and prevented the limitation of myocardial infarct size afforded by GSK360A in excised hearts (*Figure 5C***,** Supplementary material online, *Figure S4*). In accordance with the earlier results observed in HL-1 cells, hearts with smaller myocardial infarct size had lesser oxidative stress as assessed by protein carbonylation levels (*Figure 5E*) and higher mitochondrial NAD^+ levels indicating lesser mitochondrial damage (*Figure 5F*). By contrast, treatment of these hearts with HKII-peptide reversed the protective effects of GSK360A on mitochondrial function suggesting that HKII is an important downstream effector of HIF-1 in limiting oxidative stress and preventing MPTP opening following IRI (*Figure 5E and 5F*). To extend the results obtained from intact hearts to a subcellular level, we isolated cardiac mitochondria from adult rat cardiomyocytes pre-treated with 50 μM of GSK360A (Supplementary material online, *Figures S5*) before being subjected to IRI. We subsequently measured production of oxidative stress in these mitochondria using MitoSOX Red as well as MPTP opening using calcium overloading whereby the rate of mitochondrial swelling was evaluated by light scattering and decreases in the absorbance reflect passive swelling of the mitochondrial matrix. Consistent with earlier results, mitochondria isolated from cardiomyocytes treated with GSK360A generated significantly lesser superoxide compared to controls, and this reduction was duly abolished upon pre-treatment with the HKII peptide (*Figure 5G*). Simulated IRI-induced decreases in absorbance reflecting MPTP opening were also significantly inhibited in GSK360A-treated isolated mitochondria compared with DMSO, upon which was abolished in HKII-peptide-treated isolated mitochondria (*Figure*

5H), suggesting that normoxic stabilisation of HIF-1 acts directly on mitochondria by reducing oxidative stress thus preventing simulated IRI-induced MPTP opening. Notably, colocalization staining of intact adult rat cardiomyocytes for HKII and COX IV, a mitochondrial marker, revealed that the extent of mitochondrial integrity correlates directly with the binding of HKII to mitochondria (Supplementary material online, *Figures S6*) further confirming the importance of mitochondrial HKII in HIF-1-mediated cardioprotection.

3.5 Stabilising myocardial HIF-1 by genetic ablation of cardiac VHL protects the murine heart against in vivo IRI

Finally, we used cardiac-specific ablation of VHL as a genetic model to stabilise myocardial HIF-1 to ensure the aforementioned protective effects were specific to HIF-1 stabilisation and not due to PHD inhibition. The schematic diagram of the crossing is shown in *Figure 6A*. Treatment of $VHL^{fl/fl}$; α-MHC-Cre mice with 5 days of tamoxifen resulted in significant inactivation of cardiac VHL and stabilisation of HIF-1α as determined by Western blotting (*Figure 6B*). Following vehicle or tamoxifen treatment, mice were subjected to *in vivo* myocardial IRI. The area at risk (AAR) expressed as a percentage of the left ventricular volume was comparable between all treatment groups (*Figure 6C*). However, following a lethal episode of IRI, the genetic inactivation of VHL significantly reduced the myocardial infarct size to AAR ratio compared to control animals (*Figure 6D*). To allow for a more thorough characterization, adult cardiomyocytes were also isolated from these mice following treatment with either vehicle or tamoxifen and subjected to IRI. As shown in *Figure 6E*, the percentage of cell death following IRI was reduced in adult murine cardiomyocytes in which VHL was inactivated. The improved cell survival following IRI was completely abrogated by pre-treatment with the direct HIF-1α inhibitor, NSC-134754 (*Figure 6E*). Compared to cardiomyocytes isolated from vehicle-treated mice, cardiomyocytes isolated from tamoxifen-treated mice generated lesser superoxide (*Figure 6F*) leading to inhibited MPTP opening (*Figure 6G*).

4. Discussion

A number of experimental studies have reported that normoxic HIF-1α stabilisation using non-specific pharmacological PHD inhibitors (such as cobalt chloride and desferrioxamine) or genetic manipulation of HIF-1α or PHD can protect the heart from acute IRI (reviewed in [7]). In the majority of these studies, acute HIF-1 stabilisation resulted in a delayed cardioprotective effect 12-24 hours later through the transcription and activation of known cardioprotective mediators such as EPO[20], HO-1[6] and iNOS[21]. However, it has been recently shown that acute HIF-1α stabilisation may confer early cardioprotection and it has also been suggested that HIF-1 may mediate the beneficial effects of classical ischaemic preconditioning (IPC), in which one or more cycles of brief non-lethal ischaemia and reperfusion protects against a subsequent acute myocardial infarction.[22-24]. However, despite all these studies the actual mechanism through which HIF-1α stabilisation protects the heart against IRI is unclear. In this study, we present evidence for a previously undescribed role of HIF-1 in protecting against IRI through the inhibition of MPTP opening. We demonstrated that normoxic stabilisation of HIF-1 reprogrammed cell metabolism from OXPHOS to aerobic glycolysis, decreasing the production of mitochondrial oxidative stress during IRI, thereby inhibiting MPTP opening. We also demonstrated the requirement of mitochondrial HKII as a downstream effector of HIF-1 in preventing mitochondrial dysfunction following IRI.

The production of intra-mitochondrial oxidative stress and the subsequent opening of the MPTP are important signs of mitochondrial dysfunction during IRI and are critical determinants of cardiomyocyte death. A recent study demonstrated that HIF-1α stabilisation induced by genetic PHD2 ablation in skeletal muscle reprogrammed cell metabolism from aerobic to anaerobic respiration under normoxic conditions, thereby impairing exercise capacity under normoxic conditions, but rendering the skeletal muscle resistant to IRI.[25] A similar effect was seen in neonatal cardiomyocytes with HIF-1 stabilisation arising from PHD inhibition promoting anaerobic respiration during IRI.[26] Importantly, in our study, we found that the novel PHD inhibitor, GSK360A, also reprogrammed cell metabolism from OXPHOS to aerobic glycolysis under basal conditions as evidenced by: the activation of glycolytic

protein such as PDK1 and HKII, decreased mitochondrial respiration with increased intracellular lactate production, partial mitochondrial membrane depolarization, less mitochondrial ROS production and decreased levels of anti-oxidants. This metabolic switch prior to an ischaemic insult leads to inactivity of the mitochondrial electron transport chain thereby resulting in the production of lesser intra-mitochondrial oxidative stress during myocardial ischaemia such that MPTP opening at the onset of myocardial reperfusion is inhibited.

Initial gene expression analysis of HL-1 cells demonstrated the potency of the novel specific PHD inhibitor, GSK360A in stabilising HIF-1α leading to upregulation of several of its downstream target genes including HKII. We were particularly interested in HKII, previously documented to be a direct HIF-1 target,[27] due to several reasons: 1) rate limiting enzyme in glucose metabolism[28, 29]; 2) binds to mitochondria and this binding contributes to protection against cell death[18, 30]; 3) decreases cellular levels of ROS[31] and 4) has been shown to influence cardioprotection afforded by IPC through association with mitochondria[19, 32, 33] and interestingly, our data indicate that following GSK360A treatment, there was an increase in mitochondrial HKII levels. The observation that depletion of HIF-1 prevented upregulation of its target genes despite GSK360A treatment demonstrates the specificity of GSK360A as a HIF-1 activator.

Proteomics analysis following GSK360A treatment confirmed previous reports implicating HIF-1 in mediating changes in cellular metabolism as revealed by bioinformatics analysis of differentially expressed proteins. Consistent with the proteomics findings, we found that normoxic stabilisation of HIF-1 in HL-1 cells was associated with decreased usage of the mitochondrial electron transport chain (ETC) as indicated by reduced oxygen consumption, lower mitochondrial ROS and mitochondrial membrane potential while producing extra lactate compared to DMSO-treated cells. By favouring aerobic glycolysis and reducing flow through the electron transport chain one would expect to decrease the production of oxidative stress during IRI, which is beneficial as excessive ROS is known to induce MPTP opening.[34] In keeping with this interpretation, we found that GSK360A treatment afforded HL-1 cells better tolerance

against IRI by limiting generation of oxidative stress during reperfusion hence preventing MPTP opening. The beneficial effects of HIF-1 on limiting production of oxidative stress and inhibiting MPTP opening were also observed in intact rat hearts and isolated mitochondria crucially. Of note, we observed decreased production of ROS in HL-1 cells at basal condition following normoxic HIF-1 stabilisation which we postulated to be a consequence of lesser ETC activity. This was however in contrast with previous findings showing that the use of iron chelators such as desferoxamine and ethyl-3,4-dihydroxybenzoate upregulate HIF-1 and increases generation of mitochondrial ROS which is further complicated by studies demonstrating the need for ROS in stabilising HIF-1 and affording cardioprotection.[35] One possible explanation behind these discrepancies might be due to the pharmacological mode of actions employed by these drugs. While GSK360A inhibits PHD specifically by competing with the alpha-ketoglutarate site, the aforementioned iron chelators have been reported to also mediate redox reactions such as prevention of iron cycling. DFO in the past have been reported to actually increase production of hydroxyl radicals and exert a pro-oxidant and cytotoxic action[36] and as such, caution should be exercised when evaluating potential efficacy of HIF-1 activators for future studies.

Having shown that HIF-1 induces a metabolic switch which prevents lethal ROS from priming MPTP opening; we further demonstrated that this is mediated partially through mitochondrial HKII. Compared to controls, GSK360A treatment was found to enhance mitochondrial HKII levels both before ischaemia and during reperfusion period which coincidentally correlates with the degree of protection against cell death or infarct size as measured in our *in vitro* and *in vivo* studies. Interestingly, previous studies demonstrated that IPC also invokes a biphasic activation of mitochondrial HKII pre- and post-ischaemia as seen here highlighting the similarities between HIF-1 activation and IPC.[37] Several mechanisms through which mitochondrial HKII can restrain cellular damage have been proposed.[38] Overexpression of HKII leading to mitochondrial localization can lower the level of mitochondrial ROS which protect cells against oxidative stress induced cell death. Furthermore, association of HKII with

mitochondria has been suggested to inhibit cell death by preventing the activation of the MPTP or by abrogating the activity of the proapoptotic Bcl-2 family proteins. Consistent with these reports, we have shown here that increased mitochondrial HKII lowered production of oxidative stress and inhibited MPTP opening. Association of mitochondria-HKII also reduced cell death and myocardial infarct size following IRI, and crucially these protective effects were reversed when displacement of mitochondrial HKII was forced pharmacologically.

To ensure all the aforementioned effects were due to HIF-1α stabilisation and not due to PHD inhibition, we also employed a novel method to investigate the cardioprotective effects of HIF-1α stabilisation using the genetic inactivation of VHL in mice where Cre expression was limited to cardiac tissue only and could be controlled temporally. We found that 5 days of tamoxifen treatment was enough to downregulate VHL and stabilise HIF-1α. This short-term genetic inactivation of VHL resulted in a large reduction in myocardial infarct size following *in vivo* IRI. Importantly, adult mouse cardiomyocytes isolated from these mice were also resistant to IRI by reducing oxidative stress thus preventing MPTP opening.

While the literature is replete with studies involving HIF-1's protective role against ischaemia, this is the first study to underline the role of HIF-1 in protecting the heart against acute IRI by inhibiting MPTP opening. Furthermore, we show that HIF-1 stabilisation inhibits MPTP opening by reprogramming basal cell metabolism from OXPHOS to aerobic glycolysis, such that less mitochondrial oxidative stress is produced during IRI and MPTP opening is inhibited. Finally, we implicated the HIF-1 downstream target gene, HKII, as a mediator of HIF-1 cardioprotection in a similar manner to that of IPC.

Supplementary Material

Supplementary material is available at *Cardiovascular Research* online.

Funding

S-G. Ong was funded by a Dorothy Hodgkin Postgraduate Award (Medical Research Council). We thank the British Heart Foundation (Grants RG/03/007 and FS/10/039/28270) for their continued support. This work was undertaken at University College London Hospital/University College London, which received a portion of funding from the Department of Health's National Institute of Health Research Biomedical Research Centres funding scheme.

Conflict of Interest

PHM is a Director of ReOx Ltd.

References

1. Frohlich GM, Meier P, White SK, Yellon DM, Hausenloy DJ. Myocardial reperfusion injury: looking beyond primary PCI. *Eur Heart J* 2013;**34**:1714-1722.
2. Date T, Mochizuki S, Belanger AJ, Yamakawa M, Luo Z, Vincent KA, *et al.* Expression of constitutively stable hybrid hypoxia-inducible factor-1alpha protects cultured rat cardiomyocytes against simulated ischemia-reperfusion injury. *Am J Physiol Cell Physiol* 2005;**288**:C314-320.
3. Kido M, Du L, Sullivan CC, Li X, Deutsch R, Jamieson SW, *et al.* Hypoxia-Inducible Factor 1-Alpha Reduces Infarction and Attenuates Progression of Cardiac Dysfunction After Myocardial Infarction in the Mouse. *Journal of the American College of Cardiology* 2005;**46**:2116-2124.
4. Endoh H, Kaneko T, Nakamura H, Doi K, Takahashi E. Improved cardiac contractile functions in hypoxia-reoxygenation in rats treated with low concentration Co(2+). *Am J Physiol Heart Circ Physiol* 2000;**279**:H2713-2719.
5. Xi L, Taher M, Yin C, Salloum F, Kukreja RC. Cobalt chloride induces delayed cardiac preconditioning in mice through selective activation of HIF-1alpha and AP-1 and iNOS signaling. *Am J Physiol Heart Circ Physiol* 2004;**287**:H2369-2375.
6. Ockaili R, Natarajan R, Salloum F, Fisher BJ, Jones D, Fowler AA, 3rd, *et al.* HIF-1 activation attenuates postischemic myocardial injury: role for heme oxygenase-1 in modulating microvascular chemokine generation. *Am J Physiol Heart Circ Physiol* 2005;**289**:H542-548.
7. Ong SG, Hausenloy DJ. Hypoxia-inducible factor as a therapeutic target for cardioprotection. *Pharmacol Ther* 2012;**136**:69-81.
8. Hausenloy DJ, Duchen MR, Yellon DM. Inhibiting mitochondrial permeability transition pore opening at reperfusion protects against ischaemia-reperfusion injury. *Cardiovasc Res* 2003;**60**:617-625.
9. Hausenloy DJ, Maddock HL, Baxter GF, Yellon DM. Inhibiting mitochondrial permeability transition pore opening: a new paradigm for myocardial preconditioning? *Cardiovasc Res* 2002;**55**:534-543.
10. Argaud L, Gateau-Roesch O, Muntean D, Chalabreysse L, Loufouat J, Robert D, *et al.* Specific inhibition of the mitochondrial permeability transition prevents lethal reperfusion injury. *J Mol Cell Cardiol* 2005;**38**:367-374.
11. Piot C, Croisille P, Staat P, Thibault H, Rioufol G, Mewton N, *et al.* Effect of cyclosporine on reperfusion injury in acute myocardial infarction. *N Engl J Med* 2008;**359**:473-481.
12. Hausenloy DJ, Lim SY, Ong SG, Davidson SM, Yellon DM. Mitochondrial cyclophilin-D as a critical mediator of ischaemic preconditioning. *Cardiovasc Res* 2010;**88**:67-74.
13. Claycomb WC, Lanson NA, Jr., Stallworth BS, Egeland DB, Delcarpio JB, Bahinski A, *et al.* HL-1 cells: a cardiac muscle cell line that contracts and retains phenotypic characteristics of the adult cardiomyocyte. *Proc Natl Acad Sci U S A* 1998;**95**:2979-2984.
14. Smith CC, Dixon RA, Wynne AM, Theodorou L, Ong SG, Subrayan S, *et al.* Leptin-induced cardioprotection involves JAK/STAT signaling that may be linked to the mitochondrial permeability transition pore. *Am J Physiol Heart Circ Physiol* 2010;**299**:H1265-1270.
15. Kim JW, Tchernyshyov I, Semenza GL, Dang CV. HIF-1-mediated expression of pyruvate dehydrogenase kinase: a metabolic switch required for cellular adaptation to hypoxia. *Cell Metab* 2006;**3**:177-185.
16. Papandreou I, Cairns RA, Fontana L, Lim AL, Denko NC. HIF-1 mediates adaptation to hypoxia by actively downregulating mitochondrial oxygen consumption. *Cell Metab* 2006;**3**:187-197.
17. Pescador N, Villar D, Cifuentes D, Garcia-Rocha M, Ortiz-Barahona A, Vazquez S, *et al.* Hypoxia promotes glycogen accumulation through hypoxia inducible factor (HIF)-mediated induction of glycogen synthase 1. *PLoS One* 2010;**5**:e9644.

18. Chiara F, Castellaro D, Marin O, Petronilli V, Brusilow WS, Juhaszova M, *et al.* Hexokinase II detachment from mitochondria triggers apoptosis through the permeability transition pore independent of voltage-dependent anion channels. *PLoS One* 2008;**3**:e1852.
19. Wu R, Smeele KM, Wyatt E, Ichikawa Y, Eerbeek O, Sun L, *et al.* Reduction in hexokinase II levels results in decreased cardiac function and altered remodeling after ischemia/reperfusion injury. *Circ Res* 2011;**108**:60-69.
20. Cai Z, Manalo DJ, Wei G, Rodriguez ER, Fox-Talbot K, Lu H, *et al.* Hearts from rodents exposed to intermittent hypoxia or erythropoietin are protected against ischemia-reperfusion injury. *Circulation* 2003;**108**:79-85.
21. Natarajan R, Salloum FN, Fisher BJ, Kukreja RC, Fowler AA, 3rd. Hypoxia inducible factor-1 activation by prolyl 4-hydroxylase-2 gene silencing attenuates myocardial ischemia reperfusion injury. *Circ Res* 2006;**98**:133-140.
22. Eckle T, K 枚 hler D, Lehmann R, El Kasmi KC, Eltzschig HK. Hypoxia-Inducible Factor-1 Is Central to Cardioprotection: A New Paradigm for Ischemic Preconditioning. *Circulation* 2008;**118**:166-175.
23. Sarkar K, Cai Z, Gupta R, Parajuli N, Fox-Talbot K, Darshan MS, *et al.* Hypoxia-inducible factor 1 transcriptional activity in endothelial cells is required for acute phase cardioprotection induced by ischemic preconditioning. *Proc Natl Acad Sci U S A* 2012;**109**:10504-10509.
24. Cai Z, Zhong H, Bosch-Marce M, Fox-Talbot K, Wang L, Wei C, *et al.* Complete loss of ischaemic preconditioning-induced cardioprotection in mice with partial deficiency of HIF-1 alpha. *Cardiovasc Res* 2008;**77**:463-470.
25. Aragones J, Schneider M, Van Geyte K, Fraisl P, Dresselaers T, Mazzone M, *et al.* Deficiency or inhibition of oxygen sensor Phd1 induces hypoxia tolerance by reprogramming basal metabolism. *Nat Genet* 2008;**40**:170-180.
26. Sridharan V, Guichard J, Li CY, Muise-Helmericks R, Beeson CC, Wright GL. O(2)-sensing signal cascade: clamping of O(2) respiration, reduced ATP utilization, and inducible fumarate respiration. *Am J Physiol Cell Physiol* 2008;**295**:C29-37.
27. Kim JW, Gao P, Liu YC, Semenza GL, Dang CV. Hypoxia-inducible factor 1 and dysregulated c-Myc cooperatively induce vascular endothelial growth factor and metabolic switches hexokinase 2 and pyruvate dehydrogenase kinase 1. *Mol Cell Biol* 2007;**27**:7381-7393.
28. Mathupala SP, Rempel A, Pedersen PL. Glucose catabolism in cancer cells: identification and characterization of a marked activation response of the type II hexokinase gene to hypoxic conditions. *J Biol Chem* 2001;**276**:43407-43412.
29. Semenza GL. Regulation of oxygen homeostasis by hypoxia-inducible factor 1. *Physiology (Bethesda)* 2009;**24**:97-106.
30. Majewski N, Nogueira V, Bhaskar P, Coy PE, Skeen JE, Gottlob K, *et al.* Hexokinase-mitochondria interaction mediated by Akt is required to inhibit apoptosis in the presence or absence of Bax and Bak. *Mol Cell* 2004;**16**:819-830.
31. Pasdois P, Parker JE, Griffiths EJ, Halestrap AP. The role of oxidized cytochrome c in regulating mitochondrial reactive oxygen species production and its perturbation in ischaemia. *Biochem J* 2011;**436**:493-505.
32. Smeele KM, Southworth R, Wu R, Xie C, Nederlof R, Warley A, *et al.* Disruption of hexokinase II-mitochondrial binding blocks ischemic preconditioning and causes rapid cardiac necrosis. *Circ Res* 2009;**108**:1165-1169.
33. Smeele KM, Southworth R, Wu R, Xie C, Nederlof R, Warley A, *et al.* Disruption of hexokinase II-mitochondrial binding blocks ischemic preconditioning and causes rapid cardiac necrosis. *Circ Res* 2011;**108**:1165-1169.
34. Halestrap AP, Clarke SJ, Javadov SA. Mitochondrial permeability transition pore opening during myocardial reperfusion--a target for cardioprotection. *Cardiovasc Res* 2004;**61**:372-385.

35. Philipp S, Cui L, Ludolph B, Kelm M, Schulz R, Cohen MV, *et al.* Desferoxamine and ethyl-3,4-dihydroxybenzoate protect myocardium by activating NOS and generating mitochondrial ROS. *Am J Physiol Heart Circ Physiol* 2006;**290**:H450-457.
36. Borg DC, Schaich KM. Prooxidant action of desferrioxamine: Fenton-like production of hydroxyl radicals by reduced ferrioxamine. *J Free Radic Biol Med* 1986;**2**:237-243.
37. Gurel E, Smeele KM, Eerbeek O, Koeman A, Demirci C, Hollmann MW, *et al.* Ischemic preconditioning affects hexokinase activity and HKII in different subcellular compartments throughout cardiac ischemia-reperfusion. *J Appl Physiol* 2009;**106**:1909-1916.
38. Nederlof R, Eerbeek O, Hollmann MW, Southworth R, Zuurbier CJ. Targeting Hexokinase II to mitochondria to modulate energy metabolism and reduce ischemia-reperfusion injury in heart. *Br J Pharmacol* 2013.

Figure Legends

Figure 1 Treatment of HL-1 cells with GSK360A leads to normoxic stabilisation of HIF-1 and its target genes. Gene expression of HIF-1 target genes was measured following varying durations of GSK360A treatment (A). Immunoblotting of HIF-1 was performed on whole cell lysate whereas immunoblotting of HKII was performed on purified mitochondrial fraction (B) following 8 hours of GSK360A treatment. Knockdown of HIF-1 prevented upregulation of its target genes despite GSK360A treatment (C). N=5 for gene expression analysis, N=4 for immunoblotting, *P<0.05 vs DMSO control.

Figure 2 Normoxic stabilisation of HIF-1 promotes metabolic switching to aerobic glycolysis. Schematic workflow of relative quantitative proteomics on HL-1 cells treated with either DMSO or GSK360A for 8 hours (A). Bioinformatics analysis of differentially expressed proteins revealed significant changes in metabolic pathways (B). Representative time-resolved fluorometry measurement of oxygen consumption in HL-1 cells treated with or without GSK360A at 37°C (C). O_2 consumption of GSK360A-treated versus control cells for each time point was measured by linear regression in order to calculate the slopes. O_2 consumption was also measured in cells which had either HIF-1 or HKII knockdown (D). Reduced O_2 consumption expressed as percentage of DMSO-treated cells (E). N=3 for proteomics analysis, N=4 for O_2 consumption measurements, *P<0.05 vs DMSO control.

Figure 3 Aerobic glycolysis is associated with decreased usage of mitochondrial electron transport chain in HL-1 cells. Basal mitochondrial membrane potential following GSK360A treatment was measured using TMRE at 37°C (A). Basal mitochondrial ROS following GSK360A treatment was measured using Mitotracker Red CM-H_2XRos (MTR) at 37°C (B). Reduced expression of antioxidant-encoding genes following GSK360A treatment was observed (C). Measurement of intracellular lactate production was performed following GSK360A treatment (D). Periodic-acid Schiff staining of glycogen and intracellular

glycogen production were performed following GSK360A treatment (E). N≥4, *P<0.05 vs DMSO control.

Figure 4 Normoxic stabilisation of HIF-1 prevents cell death in HL-1 cells following *in vitro* simulated ischaemia-reperfusion injury (SIRI). HL-1 cells transfected with or without siRNA followed by GSK360A treatment were subjected to SIRI before determination of cell death (A) Mitochondrial fractions of each group were collected following 30 minutes of reperfusion and subjected to immunoblotting of HKII (B). Production of mitochondrial ROS (C) and MPTP opening (D) were measured at either 15 or 30 minutes of reperfusion respectively. N=6 for cell death, ROS and MPTP assays, N=4 for immunoblotting, *P<0.05 vs DMSO control.

Figure 5 GSK360A protects rat hearts against SIRI. Immunostaining of HIF-1 in hearts isolated from rats administered GSK360A 4 hours before (A). Measurement of area at risk (B) and infarct size (C) in hearts following SIRI with or without GSK360A treatment. Protein oxidation (D) and mitochondrial NAD^+ (E) following SIRI were also measured. Effects of GSK360A treatment on ROS production (F) and MPTP opening (G) were also determined by MitoSOX or mitochondrial swelling assay in isolated cardiac mitochondria. N=3 for immunostaining, N≥6 for infarct size, protein oxidation, mitochondrial NAD^+ measurements and isolated mitochondria studies, *P<0.05 vs respective controls.

Figure 6 Genetic stabilisation of HIF-1 protects against SIRI by decreasing oxidative stress thus preventing MPTP opening. Schematic diagram depicting the creation of cardiac specific $VHL^{fl/fl}$; α-MHC-Cre mice (A). Immunoblotting of VHL and HIF-1 (B). Measurement of area at risk (C) and infarct size (D) in an *in vivo* murine LAD model. Cell death in isolated adult mouse cardiomyocytes from control and transgenic mice subjected to SIRI was determined (E). Measurement of mitochondrial ROS (F) and

MPTP opening (G) were also determined in control and transgenic adult mouse cardiomyocytes following SIRI. N=3 for immunoblotting, $N \geq 6$ for infarct size and in vitro experiments, *$P<0.05$.

Figure(s)

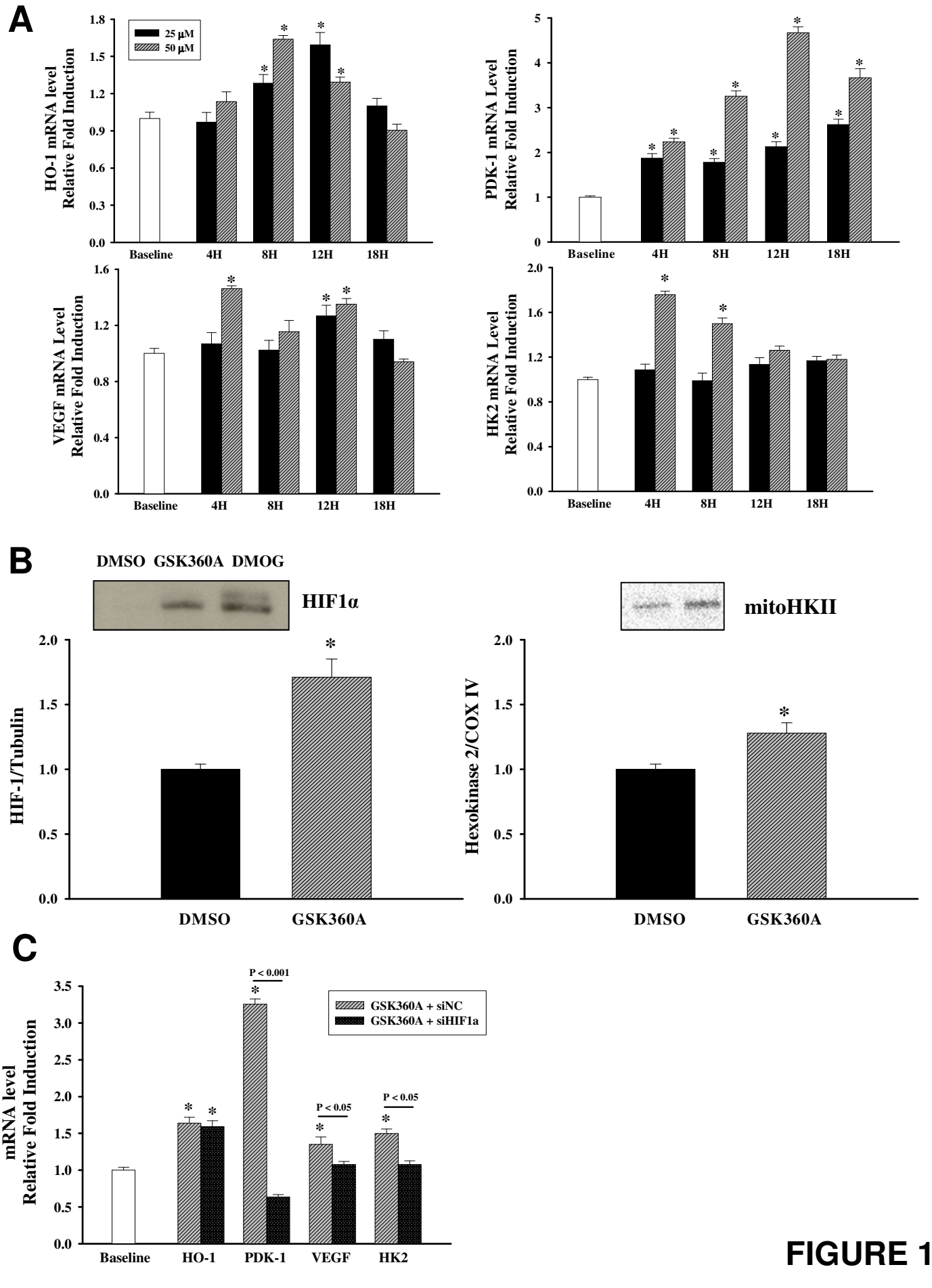

FIGURE 1

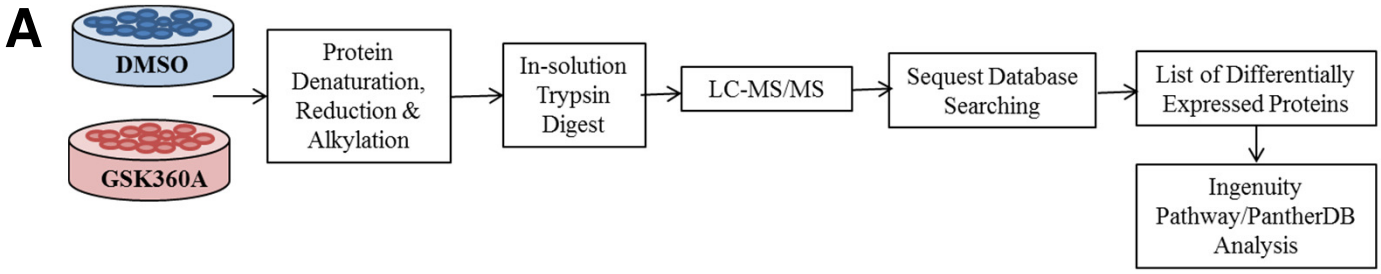
A
DMSO
GSK360A
Protein Denaturation, Reduction & Alkylation
In-solution Trypsin Digest
LC-MS/MS
Sequest Database Searching
List of Differentially Expressed Proteins
Ingenuity Pathway/PantherDB Analysis

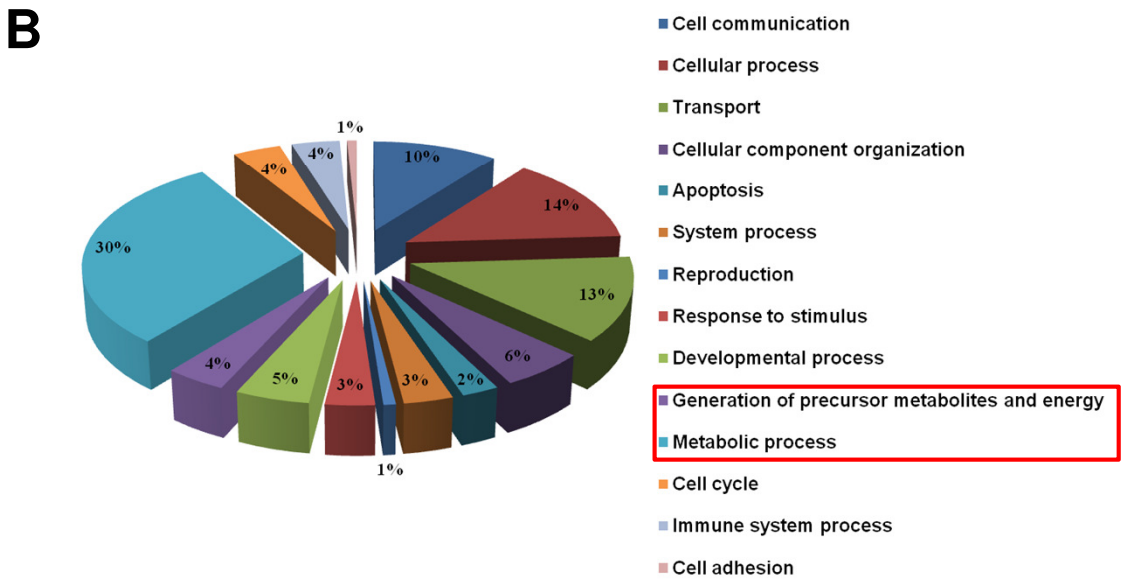
B
Cell communication
Cellular process
Transport
Cellular component organization
Apoptosis
System process
Reproduction
Response to stimulus
Developmental process
Generation of precursor metabolites and energy
Metabolic process
Cell cycle
Immune system process
Cell adhesion
10%
14%
13%
6%
2%
3%
3%
5%
4%
30%
4%
4%
1%
1%

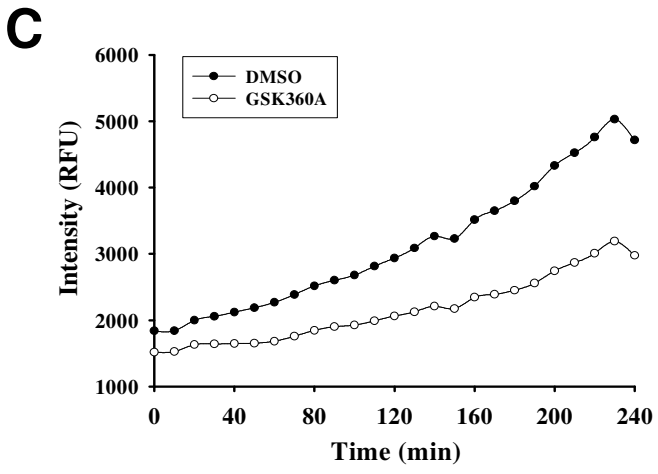
C
DMSO
GSK360A
Intensity (RFU)
Time (min)
6000
5000
4000
3000
2000
1000
0
40
80
120
160
200
240

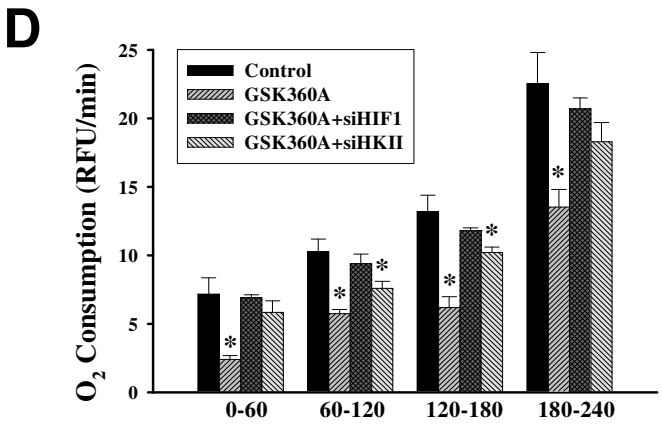
D
Control
GSK360A
GSK360A+siHIF1
GSK360A+siHKII
O2 Consumption (RFU/min)
25
20
15
10
5
0
0-60
60-120
120-180
180-240

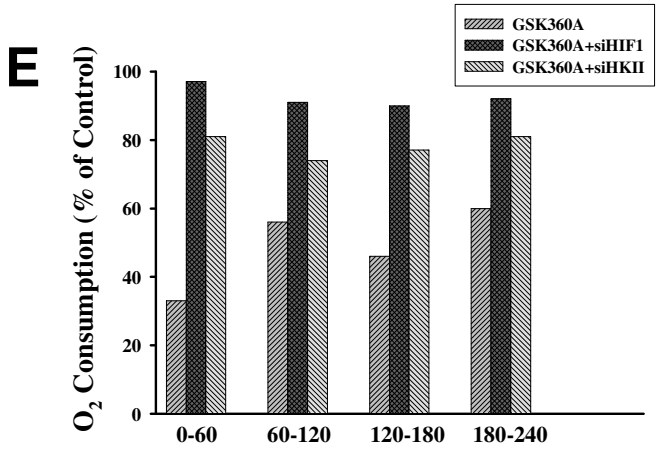
E
GSK360A
GSK360A+siHIF1
GSK360A+siHKII
O2 Consumption (% of Control)
100
80
60
40
20
0
0-60
60-120
120-180
180-240

FIGURE 2

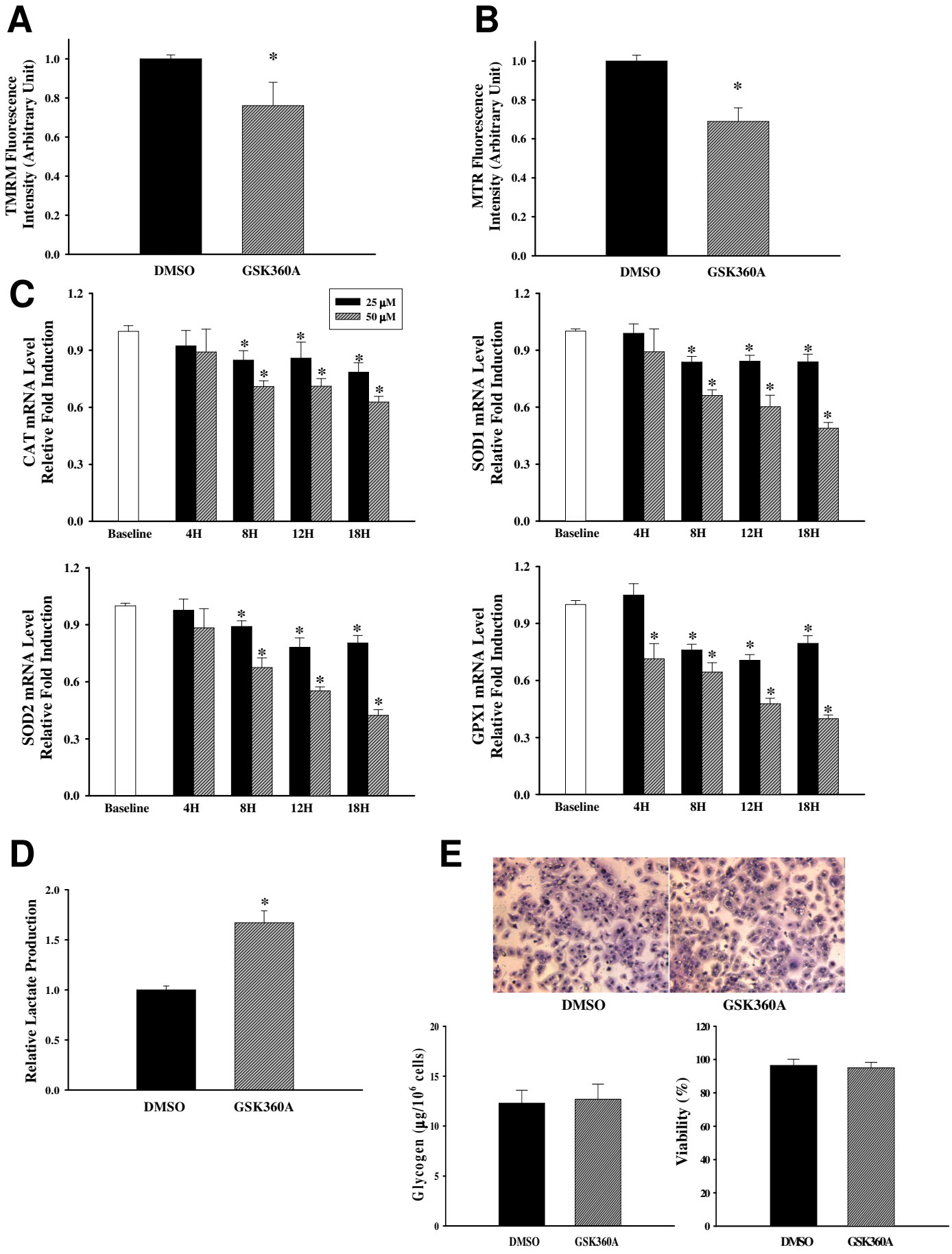
A
TMRM Fluorescence Intensity (Arbitrary Unit)
1.0
0.8
0.6
0.4
0.2
0.0
*
DMSO
GSK360A
B
MTR Fluorescence Intensity (Arbitrary Unit)
1.0
0.8
0.6
0.4
0.2
0.0
*
DMSO
GSK360A
C
CAT mRNA Level Relative Fold Induction
1.2
0.9
0.6
0.3
0.0
25 μM
50 μM
*
Baseline
4H
8H
12H
18H
SOD1 mRNA Level Relative Fold Induction
1.2
0.9
0.6
0.3
0.0
*
Baseline
4H
8H
12H
18H
SOD2 mRNA Level Relative Fold Induction
1.2
0.9
0.6
0.3
0.0
*
Baseline
4H
8H
12H
18H
GPX1 mRNA Level Relative Fold Induction
1.2
0.9
0.6
0.3
0.0
*
Baseline
4H
8H
12H
18H
D
Relative Lactate Production
2.0
1.5
1.0
0.5
0.0
*
DMSO
GSK360A
E
DMSO
GSK360A
Glycogen (μg/10^6 cells)
20
15
10
5
0
DMSO
GSK360A
Viability (%)
120
100
80
60
40
20
0
DMSO
GSK360A

FIGURE 3

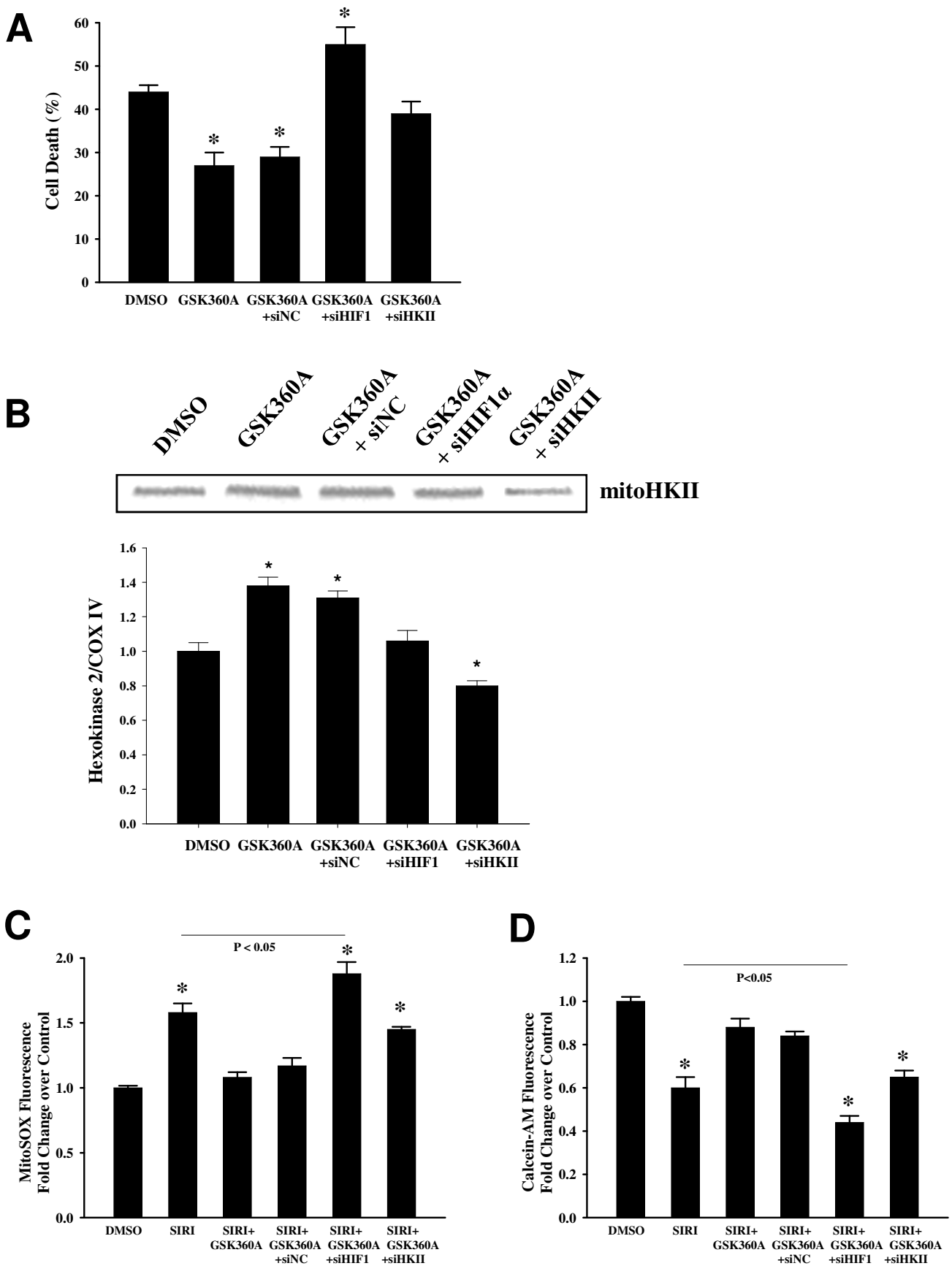
A
Cell Death (%)
60
50
40
30
20
10
0
DMSO
GSK360A
GSK360A +siNC
GSK360A +siHIF1
GSK360A +siHKII
B
DMSO
GSK360A
GSK360A + siNC
GSK360A + siHIF1α
GSK360A + siHKII
mitoHKII
Hexokinase 2/COX IV
1.6
1.4
1.2
1.0
0.8
0.6
0.4
0.2
0.0
C
P < 0.05
MitoSOX Fluorescence Fold Change over Control
2.0
1.5
1.0
0.5
0.0
DMSO
SIRI
SIRI+ GSK360A
SIRI+ GSK360A +siNC
SIRI+ GSK360A +siHIF1
SIRI+ GSK360A +siHKII
D
P<0.05
Calcein-AM Fluorescence Fold Change over Control
1.2
1.0
0.8
0.6
0.4
0.2
0.0
DMSO
SIRI
SIRI+ GSK360A
SIRI+ GSK360A +siNC
SIRI+ GSK360A +siHIF1
SIRI+ GSK360A +siHKII

FIGURE 4

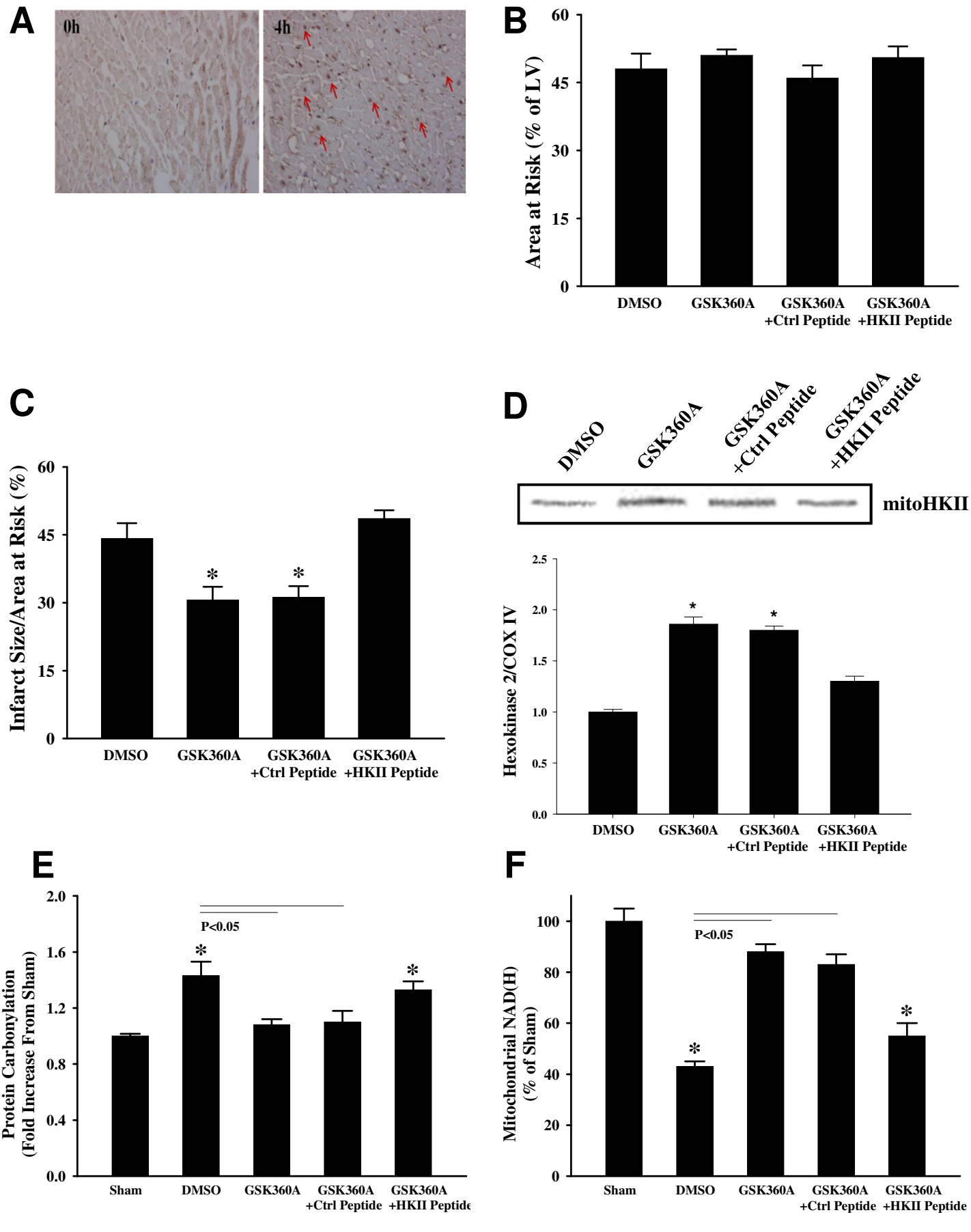
A
0h
4h
B
Area at Risk (% of LV)
60
45
30
15
0
DMSO
GSK360A
GSK360A +Ctrl Peptide
GSK360A +HKII Peptide
C
Infarct Size/Area at Risk (%)
60
45
30
15
0
*
*
DMSO
GSK360A
GSK360A +Ctrl Peptide
GSK360A +HKII Peptide
D
DMSO
GSK360A
GSK360A +Ctrl Peptide
GSK360A +HKII Peptide
mitoHKII
Hexokinase 2/COX IV
2.5
2.0
1.5
1.0
0.5
0.0
*
*
DMSO
GSK360A
GSK360A +Ctrl Peptide
GSK360A +HKII Peptide
E
Protein Carbonylation (Fold Increase From Sham)
2.0
1.6
1.2
0.8
0.4
0.0
P<0.05
*
*
Sham
DMSO
GSK360A
GSK360A +Ctrl Peptide
GSK360A +HKII Peptide
F
Mitochondrial NAD(H) (% of Sham)
100
80
60
40
20
0
P<0.05
*
*
Sham
DMSO
GSK360A
GSK360A +Ctrl Peptide
GSK360A +HKII Peptide

FIGURE 5

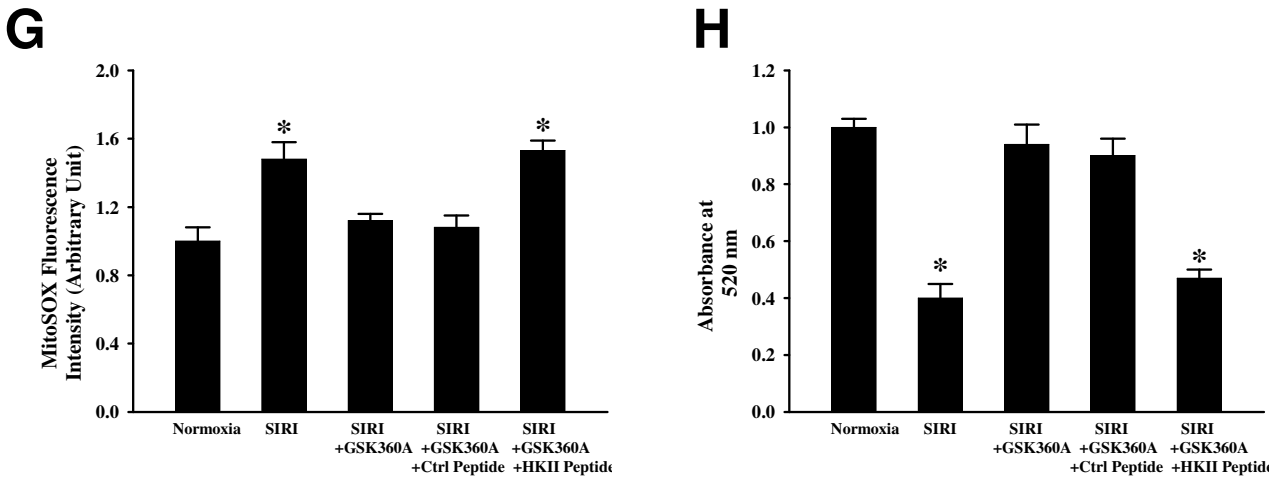

FIGURE 5 Cont'd

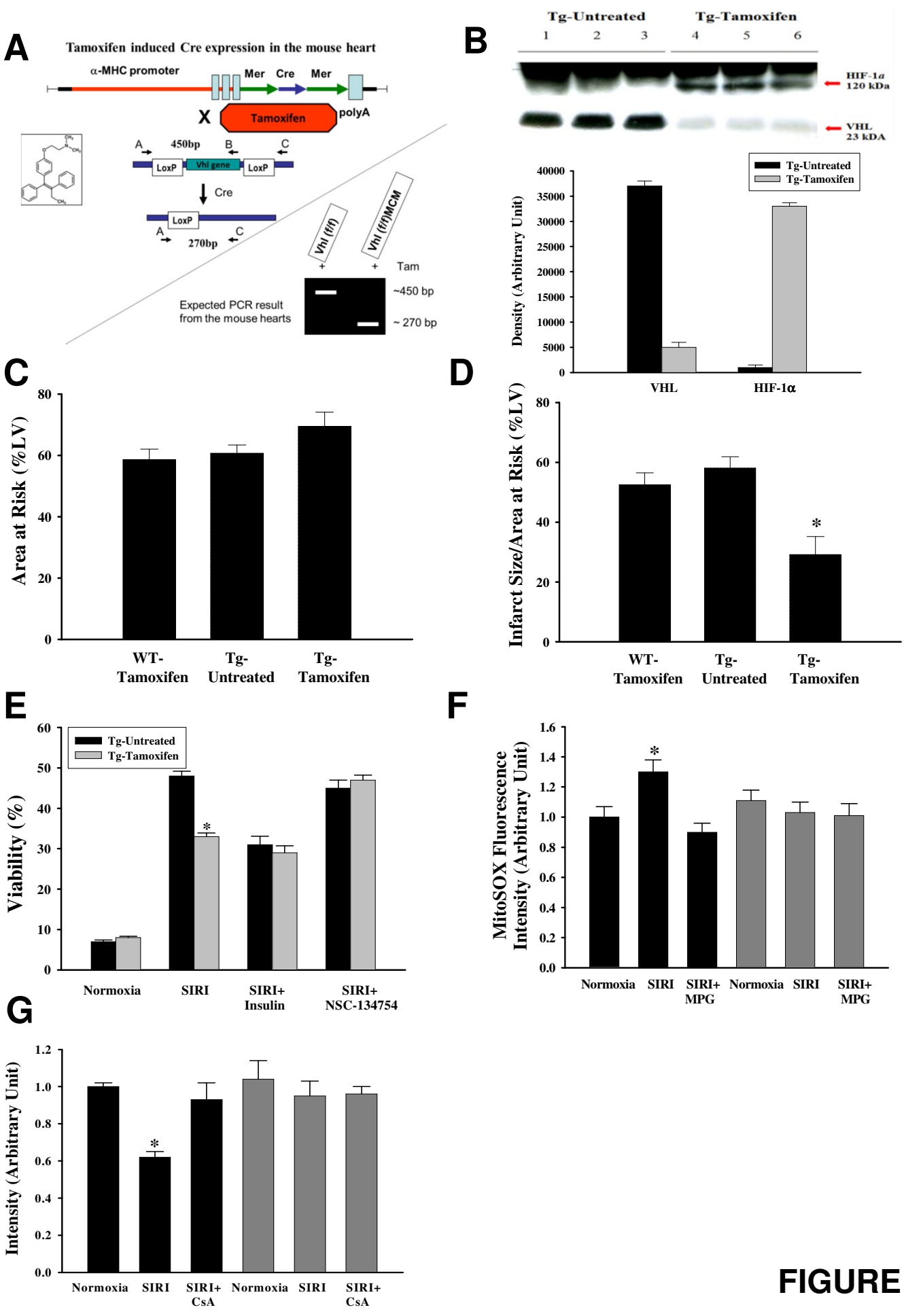
A
Tamoxifen induced Cre expression in the mouse heart
α-MHC promoter
Mer
Cre
Mer
X
Tamoxifen
polyA
A
450bp
B
C
LoxP
Vhl gene
LoxP
Cre
LoxP
A
C
270bp
Vhl (f/f)
Vhl (f/f)MCM
+
+
Tam
Expected PCR result
from the mouse hearts
~450 bp
~ 270 bp
B
Tg-Untreated
Tg-Tamoxifen
1
2
3
4
5
6
HIF-1α
120 kDa
VHL
23 kDA
Tg-Untreated
Tg-Tamoxifen
Density (Arbitrary Unit)
40000
35000
30000
25000
20000
15000
10000
5000
0
VHL
HIF-1α
C
Area at Risk (%LV)
80
60
40
20
0
WT-
Tamoxifen
Tg-
Untreated
Tg-
Tamoxifen
D
Infarct Size/Area at Risk (%LV)
80
60
40
20
0
*
WT-
Tamoxifen
Tg-
Untreated
Tg-
Tamoxifen
E
Tg-Untreated
Tg-Tamoxifen
Viability (%)
60
50
40
30
20
10
0
*
Normoxia
SIRI
SIRI+
Insulin
SIRI+
NSC-134754
F
MitoSOX Fluorescence
Intensity (Arbitrary Unit)
1.6
1.4
1.2
1.0
0.8
0.6
0.4
0.2
0.0
*
Normoxia
SIRI
SIRI+
MPG
Normoxia
SIRI
SIRI+
MPG
G
Calcein-AM Fluorescence
Intensity (Arbitrary Unit)
1.2
1.0
0.8
0.6
0.4
0.2
0.0
*
Normoxia
SIRI
SIRI+
CsA
Normoxia
SIRI
SIRI+
CsA

FIGURE 6

SUPPLEMENTAL MATERIAL

HIF-1 reduces myocardial ischemia-reperfusion injury by targeting the mitochondria permeability transition pore

Sang-Ging Ong[1,5]; Won Hee Lee[2,5]; Louisa Theodorou[1]; Kazuki Kodo[2]; Shiang Y Lim[1]; Deepa H Shukla[3]; Thomas Briston[3]; Serafim Kiriakidis[4]; Margaret Ashcroft[3]; Sean M Davidson[1]; Patrick H Maxwell[3]; Derek M Yellon[1]; Derek J Hausenloy[1]

[1]The Hatter Cardiovascular Institute, University College London & Medical School, UK. [2]Department of Medicine, Division of Cardiology, Stanford University, Stanford, USA. [3]Centre for Cell Signalling and Molecular Genetics, University College London & Medical School, UK. [4]Kennedy Institute of Rheumatology, NDORMS, University of Oxford, UK.

[5]These authors contributed equally.

SUPPLEMENTAL METHODS

Quantitative Real-Time PCR

Total RNA was isolated from HL-1 cells treated with either DMSO, siRNAs or GSK360A using RNeasy Mini Kit (Qiagen) according to manufacturer's instructions. Total RNA was reverse transcribed with oligo (dT) primers using the SuperScript first-strand synthesis system for RT-PCR (Applied Biosystems). All siRNAs, PCR primers and Taqman probes were obtained from Applied Biosystems. Reactions were analyzed using the ABI Prism 7300 sequence detection system and data were normalized to GAPDH levels and quantified using the comparative threshold cycle (C_t) method.

Oxygen Consumption

Oxygen consumption was monitored using the fluorescent oxygen probe MitoXpress-Xtra-HS. HL-1 cells (2×10^4) were seeded on a 96-well plate and left to incubate overnight. On the day of experiment, cells were washed and replaced with medium containing either DMSO or GSK360A. In a separate set of experiments, seeded cells were treated with negative control siRNA or siHIF1 or siHKII for 24 hours before being treated with either DMSO or GSK360A. The oxygen sensitive probe was added to each well and all wells were overlaid with mineral oil. Oxygen consumption was monitored as a function of fluorescence (excitation/emission 380/650 nm) every 3 minutes over a 4 hours period on a time-resolved fluorescence microplate reader (Tecan, Infinite M1000). Rate of oxygen consumption was determined from the slope of fluorescence versus a specific time frame for GSK360A-treated cells and vehicle-treated cells using arbitrary units.

Mitochondrial Isolation

Mitochondria were isolated from HL-1 cells using Mitochondria Isolation Kit for Cultured Cells (Thermo Scientific) and from heart tissue using Mitochondria Isolation Kit for Tissue (Thermo Scientific) according to manufacturer's instructions. Briefly, cells or heart pieces were homogenized with a 2-mL Dounce homogeniser. Homogenates were then added to Buffer C with protease inhibitors. Nuclei were

pelleted at 700g for 10 minutes. Supernatants were placed into a new tube, and cytosolic and mitochondrial fractions were separated by differential centrifugation at 6000g for 15 minutes. Mitochondrial pellets were then re-suspended or frozen for subsequent use.

Immunoblotting

Immunoblotting was performed with HIF-1α (1:1000, Novus Biologicals), hexokinase II (1:1000, Cell Signaling), α-tubulin (1:1000, Cell Signaling) and COX IV (1:1000, Cell Signaling). Ten micrograms of protein were loaded. Expression was normalised to α-tubulin for whole cell lysate and to COX IV for mitochondrial fraction for loading differences. Densitometry analysis was performed using Image J.

Intracellular Lactate and Glycogen Measurements

HL-1 cells (8×10^5) were seeded on a 6-well plate and left to incubate overnight. On the day of experiment, cells were washed and replaced with medium containing either DMSO or GSK360A for 8 hours. Upon completion, cells were lysed, centrifuged and supernatant was collected for intracellular lactate and glycogen measurements using Lactate Colorimetric Assay Kit II or Glycogen Colorimetric Assay Kit II (both from Biovision Inc) respectively according to manufacturer's instructions. Results were normalised against cell number as determined by trypan blue assay using the Countess Automated Cell Counter (Applied Biosystems).

Periodic acid-Schiff Staining

Staining of glycogen in HL-1 cells treated with GSK360A was performed using a Periodic acid-Schiff staining kit (Sigma-Aldrich) according to manufacturer's instructions.

Proteomic Analysis

GSK360A or DMSO-treated cells were lysed in urea buffer (8M urea, 75 mM NaCl, 50 mM Tris, pH 8.2). Lysates were centrifuged, and supernatant was collected as protein fractions. 20 μg of each sample

was reduced with 5 mM DTT at 55°C for 30 min, alkylated with 15 mM iodoacetamide at room temperature for 30 minutes in dark, diluted to 1M urea concentration followed by digestion with trypsin. LC-MS/MS analysis was performed with an Easy-nLC 1000 (Thermo Scientific) coupled to an Orbitrap Elite mass spectrometer (Thermo Scientific). The LC system configured in a vented format consisted of a fused-silica nanospray needle (PicoTip™ emitter, 50 µm ID, New Objective) packed in-house with Magic C18 AQ 100Å reverse-phase media (Michrom Bioresources Inc.) (25 cm), and a trap (IntegraFrit™ Capillary, 100 µm ID, New Objective) containing Magic C18 AQ 200Å (2 cm). The peptide sample was diluted in 10 µL of 2% acetonitrile and 0.1% formic acid in water and 8 µL was loaded onto the column and separated using a two-mobile-phase system consisting of 0.1% formic acid in water (A) and 0.1% acetic acid in acetonitrile (B). A 60-minute gradient from 7% to 35% acetonitrile in 0.1% formic acid at a flow rate of 400 nL/minute was used for chromatographic separations. The mass spectrometer was operated in a data-dependent MS/MS mode over the m/z range of 400-1800. For each cycle, the 20 most abundant ions from the scan were selected for MS/MS analysis using 35% normalized collision energy. Selected ions were dynamically excluded for 30 seconds. Tandem mass spectra were extracted by ProteomeDiscoverer software by Thermo. Charge state deconvolution and deisotoping were not performed. All MS/MS samples were analyzed using Sequest (Thermo Fisher Scientific,). Sequest was set up to search ipi_MOUSE_v3_87.fasta (unknown version, 59534 entries) assuming the digestion enzyme trypsin. Sequest was searched with a fragment ion mass tolerance of 0.80 Da and a parent ion tolerance of 10.0 PPM. Carbamidomethyl of cysteine was specified in Sequest as a fixed modification. Oxidation of methionine was specified in Sequest as a variable modification. Scaffold (version Scaffold_4.0.5, Proteome Software Inc., Portland, OR) was used to validate MS/MS based peptide and protein identifications. Peptide identifications were accepted if they could be established at greater than 95.0% probability by the Scaffold Local FDR algorithm. Protein identifications were accepted if they could be established at greater than 99.0% probability and contained at least 2 identified peptides. Protein probabilities were assigned by the Protein Prophet algorithm. Proteins that contained similar peptides and could not be differentiated based on MS/MS analysis alone were grouped to satisfy the principles of

parsimony. Proteins sharing significant peptide evidence were grouped into clusters. Proteins were annotated with GO terms from NCBI (downloaded May 22, 2013).

Isolation of adult rat and mouse ventricular cardiomyocytes

Isolated adult rat or mouse cardiomyocytes were used to investigate the effects of HIF-1α stabilisation through pharmacological or genetic means respectively. Adult rat and mouse cardiomyocytes were isolated by collagenase perfusion using previously described methods with modifications to obtain >95% rod-shaped cells. Following isolation, the cardiomyocytes were seeded onto laminin-coated 6-wells plate in M199 medium containing 10 units/mL penicillin, 10 mg/mL streptomycin and 5% fetal calf serum for incubation before use on the same day of isolation.

Measurement of NAD^+ Levels

Isolated mitochondria fractions were precipitated with perchloric acid, followed by neutralisation with potassium hydroxide. NAD^+ was then measured using a cycling reaction as previously described[2] and NAD^+ concentrations were determined by comparison to a standard curve and normalised to protein concentration as determined by a Piercenet 660nm protein assay (Thermo Scientific).

Measurement of Protein Carbonylation

Protein carbonylation levels of heart tissue homogenates were measured using Protein Carbonyl Colorimetric Assay Kit (Cayman Chemicals) according to manufacturer's instructions. Absorbance values were normalised against each sample's protein concentration.

Mitochondrial Swelling Assay

Isolated cardiomyocyte mitochondria were suspended in a swelling buffer (250 mmol/L sucrose, 10 mmol/L MOPS, 5 μmol/L EGTA, 2 mmol/L $MgCl_2$, 5 mmol/L KH_2PO_4, 5 mmol/L pyruvate and 5

mmol/L malate) and incubated with 150 μmol/L $CaCl_2$ in a final volume of 200 μL in a 96-well plate for 20 min. Absorbance was measured at 520 nm.

Statistical Analysis

The data shown are presented as the mean ± standard error of three or more independent experiments. Differences are considered statistically significant at $P<0.05$, assessed using the Student's *t* test (for paired samples) or the ANOVA test (for more than two groups) followed by post-hoc analysis using Tukey's test

ONLINE TABLE I. List of Significantly Downregulated Proteins

#	Identified Proteins (64/1610)	Accession #	MW (kDa)	FC Ratio
1	Ras GTPase-activating-like protein IQGAP1	IPI00467447	189	(0.2)
2	Cystatin-C	IPI00123744	16	(0.3)
3	Isoform 2 of Translation initiation factor eIF-2B subunit delta	IPI00221819	60	(0.3)
4	Arpc1b protein	IPI00125143	41	(0.3)
5	Spectrin beta 4 isoform sigma1	IPI00856469	289	(0.3)
6	Splicing factor, arginine/serine-rich 11 isoform 1	IPI00468994	43	(0.3)
7	Isoform 2 of Zinc finger CCCH domain-containing protein 4	IPI00625723	132	(0.3)
8	High mobility group nucleosome-binding domain-containing protein 5	IPI00311626	45	(0.3)
9	Polymerase delta-interacting protein 3	IPI00229721	46	(0.3)
10	Isoform 1 of Tether containing UBX domain for GLUT4	IPI00121364	60	(0.3)
11	Glycogen [starch] synthase, muscle	IPI00130127	84	(0.3)
12	SWI/SNF-related matrix-associated actin-dependent regulator of chromatin subfamily D	IPI00467181	55	(0.3)
13	Cluster of Keratin, type II cytoskeletal 1 (IPI00625729)	IPI00625729	66	(0.3)
14	Methionyl-tRNA synthetase, cytoplasmic	IPI00461469	101	(0.3)
15	RILP-like protein 1	IPI00121674	47	(0.3)

16	Isoform 2 of Ubiquitin carboxyl-terminal hydrolase 10	IPI00420601	87	(0.4)
17	Cluster of Mitogen-activated protein kinase 3 (IPI00230277)	IPI00230277	43	(0.4)
18	Cluster of Glutathione S-transferase Mu 2 (IPI00228820)	IPI00228820	26	(0.4)
19	Proteasome activator complex subunit 3	IPI00113660	30	(0.4)
20	Cluster of E3 ubiquitin-protein ligase TRIM63 (IPI00471257)	IPI00471257	40	(0.4)
21	Inosine triphosphate pyrophosphatase	IPI00678003	22	(0.4)
22	Cluster of Isoform 1 of Yorkie homolog (IPI00108989)	IPI00108989	52	(0.4)
23	Cluster of Nuclear receptor-binding protein (IPI00222739)	IPI00222739	60	(0.4)
24	Cytosolic non-specific dipeptidase	IPI00315879	53	(0.4)
25	Lipoprotein lipase	IPI00319188	53	(0.4)
26	Interferon regulatory factor 2 binding protein 2	IPI00357145	59	(0.4)
27	Annexin A7	IPI00114017	50	(0.4)
28	Methionine aminopeptidase	IPI00272238	54	(0.4)
29	Synaptopodin 2-like protein	IPI00226219	103	(0.4)
30	Omega-amidase NIT2	IPI00119945	31	(0.4)
31	Cluster of mRNA turnover protein 4 homolog (IPI00132578)	IPI00132578	28	(0.4)
32	Putative ribosomal RNA methyltransferase NOP2	IPI00311453	87	(0.4)
33	Myoglobin	IPI00230760	17	(0.4)
34	Isoform 1 of SOSS complex subunit C	IPI00341612	11	(0.4)
35	Probable fructose-2,6-bisphosphatase TIGAR	IPI00227451	29	(0.4)

36	Catenin beta-1	IPI00125899	85	(0.4)
37	Epididymal secretory protein E1	IPI00129186	16	(0.4)
38	Cluster of Long-chain-fatty-acid--CoA ligase 1 (IPI00112549)	IPI00112549	78	(0.4)
39	Dynactin subunit 2	IPI00116112	44	(0.4)
40	Pleiotropic regulator 1	IPI00331172	57	(0.5)
41	Ataxin-2	IPI00117229	136	(0.5)
42	Isoform 1 of Squamous cell carcinoma antigen recognized by T-cells 3	IPI00458854	110	(0.5)
43	Isoform 1 of Myosin-14	IPI00453996	229	(0.5)
44	Proteasome subunit beta type-3	IPI00314467	23	(0.5)
45	Cluster of nuclear mitotic apparatus protein 1 (IPI00263048)	IPI00263048	236	(0.5)
46	Cluster of E3 ubiquitin-protein ligase HUWE1 (IPI00463909)	IPI00463909	483	(0.5)
47	Apoptosis-associated speck-like protein containing a CARD	IPI00109709	21	(0.5)
48	Gem-associated protein 5 isoform 1	IPI00953772	167	(0.5)
49	Cysteine and histidine-rich domain-containing protein 1	IPI00134017	37	(0.5)

ONLINE TABLE II. List of Significantly Upregulated Proteins

#	Identified Proteins (92/1610)	Accession #	MW (kDa)	FC Ratio
1	Putative uncharacterized protein	IPI00338458	78	(2.0)
2	Cation-dependent mannose-6-phosphate receptor	IPI00108844	31	(2.0)
3	NADPH--cytochrome P450 reductase	IPI00621548	77	(2.0)
4	Prenylcysteine oxidase	IPI00460063	56	(2.0)
5	Lipoamide acyltransferase component of branched-chain alpha-keto acid dehydrogenase complex	IPI00130535	53	(2.0)
6	Catalase	IPI00312058	60	(2.0)
7	NADH dehydrogenase [ubiquinone] 1 beta subcomplex subunit 4	IPI00132390	15	(2.0)
8	Peptidyl-tRNA hydrolase 2, mitochondrial isoform a	IPI00153702	20	(2.0)
9	Translocon-associated protein subunit delta	IPI00122346	19	(2.0)
10	Electron transfer flavoprotein-ubiquinone oxidoreductase, mitochondrial	IPI00121322	68	(2.0)
11	Isoform 1 of ATPase family AAA domain-containing protein 3	IPI00126913	67	(2.0)
12	Cluster of Glia maturation factor, beta (IPI00467495)	IPI00467495	17	(2.0)
13	NADH dehydrogenase [ubiquinone] 1 alpha subcomplex subunit 7	IPI00130322	13	(2.0)
14	6-phosphofructokinase, liver type	IPI00554862	85	(2.0)
15	Ras-related protein Rab-21	IPI00337980	24	(2.0)
16	Vesicle-trafficking protein SEC22b	IPI00114368	25	(2.0)

17	Splicing factor 3B subunit 5	IPI00311948	10	(2.0)
18	Cluster of Isoform 1 of SUMO-activating enzyme subunit 1 (IPI00129105)	IPI00129105	39	(2.0)
19	Isoform 2 of Acidic leucine-rich nuclear phosphoprotein 32 family member B	IPI00113536	37	(2.0)
20	Mitochondrial-processing peptidase subunit beta	IPI00274656	55	(2.0)
21	Histidine triad nucleotide-binding protein 2, mitochondrial	IPI00133034	17	(2.0)
22	Isoform 1 of Nuclear factor 1 B-type	IPI00130129	64	(2.0)
23	Guanine nucleotide-binding protein G(I)/G(S)/G(O) subunit gamma-12	IPI00227838	8	(2.1)
24	Pyrroline-5-carboxylate reductase 3	IPI00153234	29	(2.1)
25	BRO1 domain-containing protein BROX	IPI00408556	46	(2.1)
26	V-type proton ATPase subunit B, brain isoform	IPI00119113	57	(2.2)
27	Lon protease homolog	IPI00319518	106	(2.2)
28	Elongation factor Ts, mitochondrial	IPI00113052	35	(2.2)
29	Maleylacetoacetate isomerase	IPI00126120	24	(2.2)
30	Isoform 1 of Presequence protease, mitochondrial	IPI00170126	117	(2.2)
31	Isoform LAMP-2A of Lysosome-associated membrane glycoprotein 2	IPI00134549	46	(2.2)
32	Uncharacterized protein C6orf125 homolog	IPI00133350	16	(2.2)
33	Guanine nucleotide-binding protein G(q) subunit alpha	IPI00228618	42	(2.2)
34	Starch-binding domain-containing protein 1	IPI00226656	36	(2.3)
35	Cluster of Calcium-binding mitochondrial carrier protein Aralar1 (IPI00308162)	IPI00308162	75	(2.3)
36	N-alpha-acetyltransferase 10, NatA catalytic subunit isoform	IPI00758413	25	(2.3)

	2			
37	Serum albumin	IPI00131695	69	(2.3)
38	Synaptic vesicle membrane protein VAT-1 homolog	IPI00126072	43	(2.3)
39	Emerin	IPI00114401	29	(2.3)
40	Transmembrane protein 55A	IPI00113239	28	(2.3)
42	Isoform 2 of Regulator of differentiation 1	IPI00975110	56	(2.3)
43	Uncharacterized protein	IPI00665734	111	(2.3)
44	Phosphoenolpyruvate carboxykinase [GTP], mitochondrial	IPI00223060	73	(2.3)
45	GMP reductase 1	IPI00121566	37	(2.4)
46	NADH dehydrogenase [ubiquinone] 1 alpha subcomplex subunit 13	IPI00230715	17	(2.4)
47	ADP-ribosylation factor 6	IPI00221616	20	(2.4)
48	Metallothionein	IPI00464347	6	(2.4)
49	Trans-2-enoyl-CoA reductase, mitochondrial	IPI00121276	40	(2.4)
50	U2 small nuclear ribonucleoprotein A'	IPI00170008	28	(2.4)
51	Serine protease HTRA2, mitochondrial	IPI00275992	49	(2.4)
52	Methylmalonate-semialdehyde dehydrogenase [acylating], mitochondrial	IPI00461964	58	(2.4)
53	Isoform 1 of Endoplasmic reticulum metallopeptidase 1	IPI00407222	100	(2.5)
54	ATPase Asna1	IPI00624501	39	(2.5)
55	Isoform 1 of Dynamin-like 120 protein, mitochondrial	IPI00117657	111	(2.5)
56	Apolipoprotein O isoform 3	IPI00670400	19	(2.6)
57	[Pyruvate dehydrogenase [lipoamide]] kinase isozyme 3, mitochondrial	IPI00123004	48	(2.7)
58	Apolipoprotein O-like	IPI00112493	29	(2.7)

59	Protein VAC14 homolog	IPI00330619	88	(2.7)
60	Isochorismatase domain-containing protein 2A, mitochondrial	IPI00757372	22	(2.8)
61	Cluster of Mitochondrial import receptor subunit TOM22 homolog (IPI00315135)	IPI00315135	16	(2.8)
62	Cluster of NADH dehydrogenase [ubiquinone] iron-sulfur protein 2, mitochondrial (IPI00128023)	IPI00128023	53	(2.8)
63	Putative uncharacterized protein	IPI00133342	14	(2.8)
64	Guanine nucleotide-binding protein subunit alpha-11	IPI00121387	42	(3.0)
65	Metaxin-1 isoform 1	IPI00112327	51	(3.0)
66	Endoplasmic reticulum resident protein 44	IPI00134058	47	(3.0)
67	Isoform 1 of Eukaryotic translation initiation factor 3 subunit K	IPI00120322	25	(3.2)
68	Isoform 2 of Ubiquitin carboxyl-terminal hydrolase 7	IPI00463367	133	(3.2)
69	Cytochrome c oxidase subunit 6C	IPI00131771	8	(3.2)
70	Membrane-associated progesterone receptor component 2	IPI00351206	23	(3.2)
71	Lanosterol 14-alpha demethylase	IPI00458711	57	(3.2)
72	2',5'-phosphodiesterase 12	IPI00420284	68	(3.4)
73	Solute carrier family 2, facilitated glucose transporter member 1	IPI00308691	54	(3.4)
74	Mitochondrial import inner membrane translocase subunit Tim23	IPI00849271	22	(3.6)
75	LETM1 and EF-hand domain-containing protein 1, mitochondrial	IPI00131177	83	(3.6)
76	Aldehyde dehydrogenase X, mitochondrial	IPI00113073	58	(4.0)

77	ATP-binding cassette sub-family B member 7, mitochondrial	IPI00672663	83	(4.0)
78	CDGSH iron-sulfur domain-containing protein 1	IPI00128346	12	(4.0)
79	Mitochondrial import receptor subunit TOM70	IPI00377728	68	(4.7)
80	Histone H4	IPI00407339	11	(5.2)
81	Cluster of Histone H3.2 (IPI00230730)	IPI00230730	15	(5.4)

SUPPLEMENTAL FIGURES

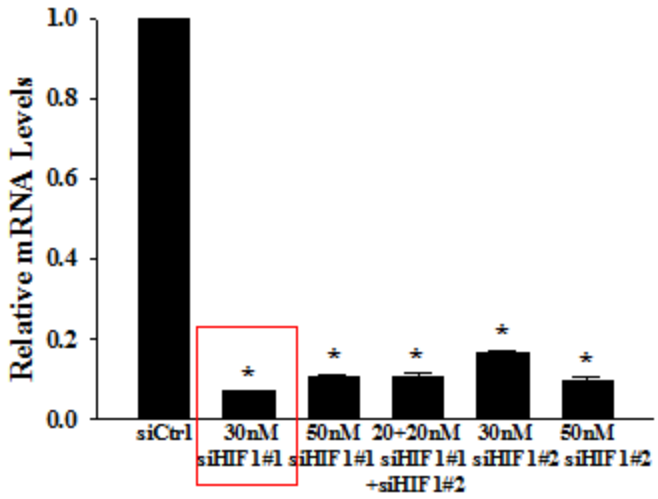

Figure S1. Efficacy testing of siRNAs against HIF-1 in HL-1 cells. N=4, P<0.05.

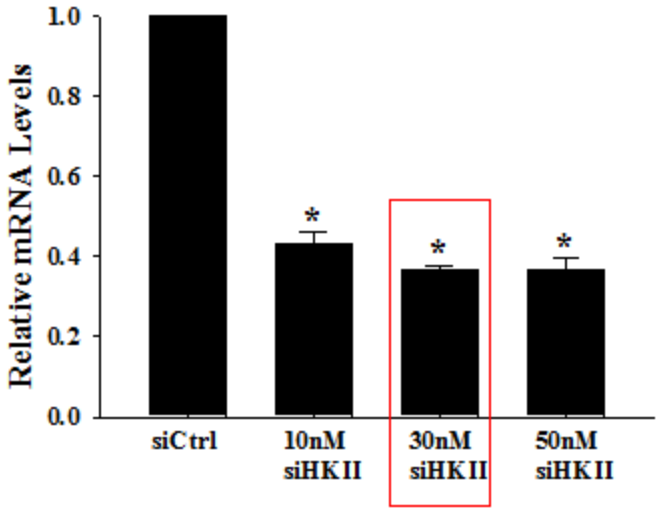

Figure S2. Efficacy testing of siRNAs against hexokinase II in HL-1 cells. N=4, P<0.05.

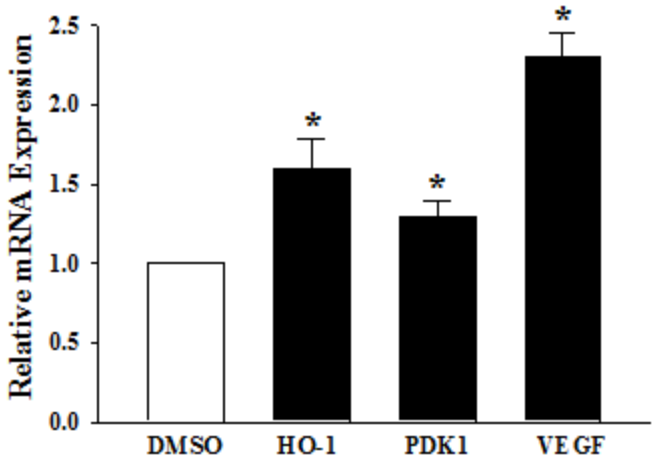

Figure S3. qPCR of HIF-1 target genes in rat hearts treated with GSK360A for 4 hours. N=4, P<0.05.

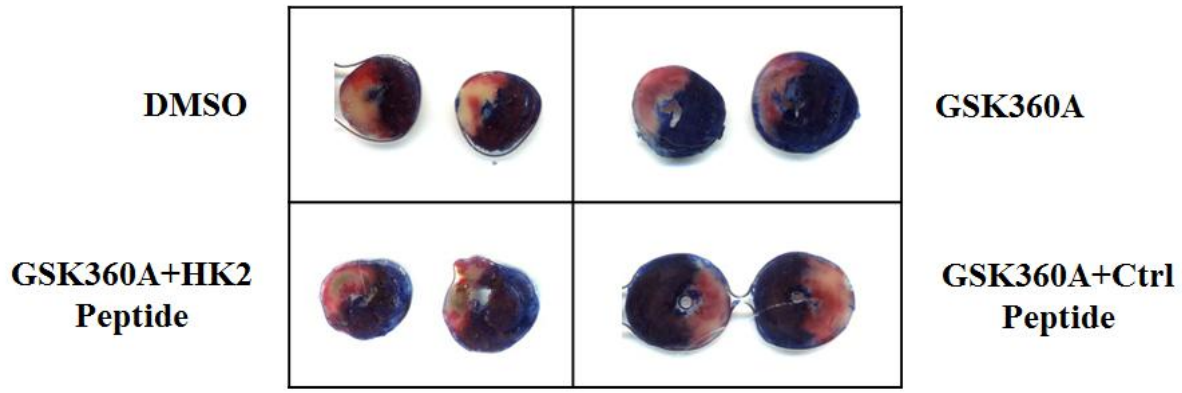

Figure S4. Representative infarct size analysis of hearts treated with GSK360A prior to simulated ischaemia-reperfusion injury.

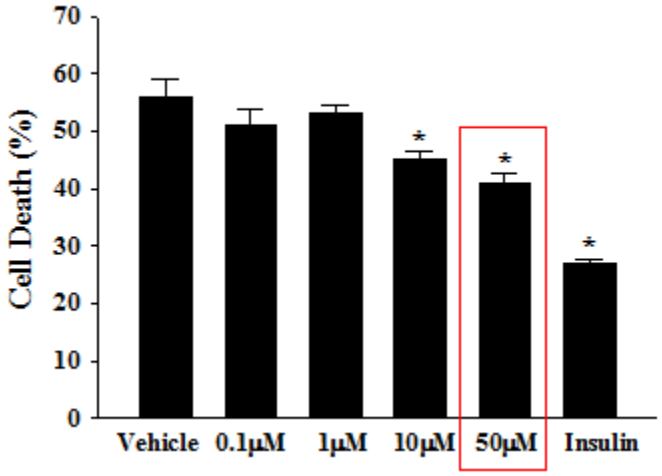

Figure S5. Adult rat cardiomyocytes were treated with different concentrations of GSK360A before being subjected to simulated ischaemia-reperfusion injury. Cell death was then measured. N=5/group, $P<0.05$.

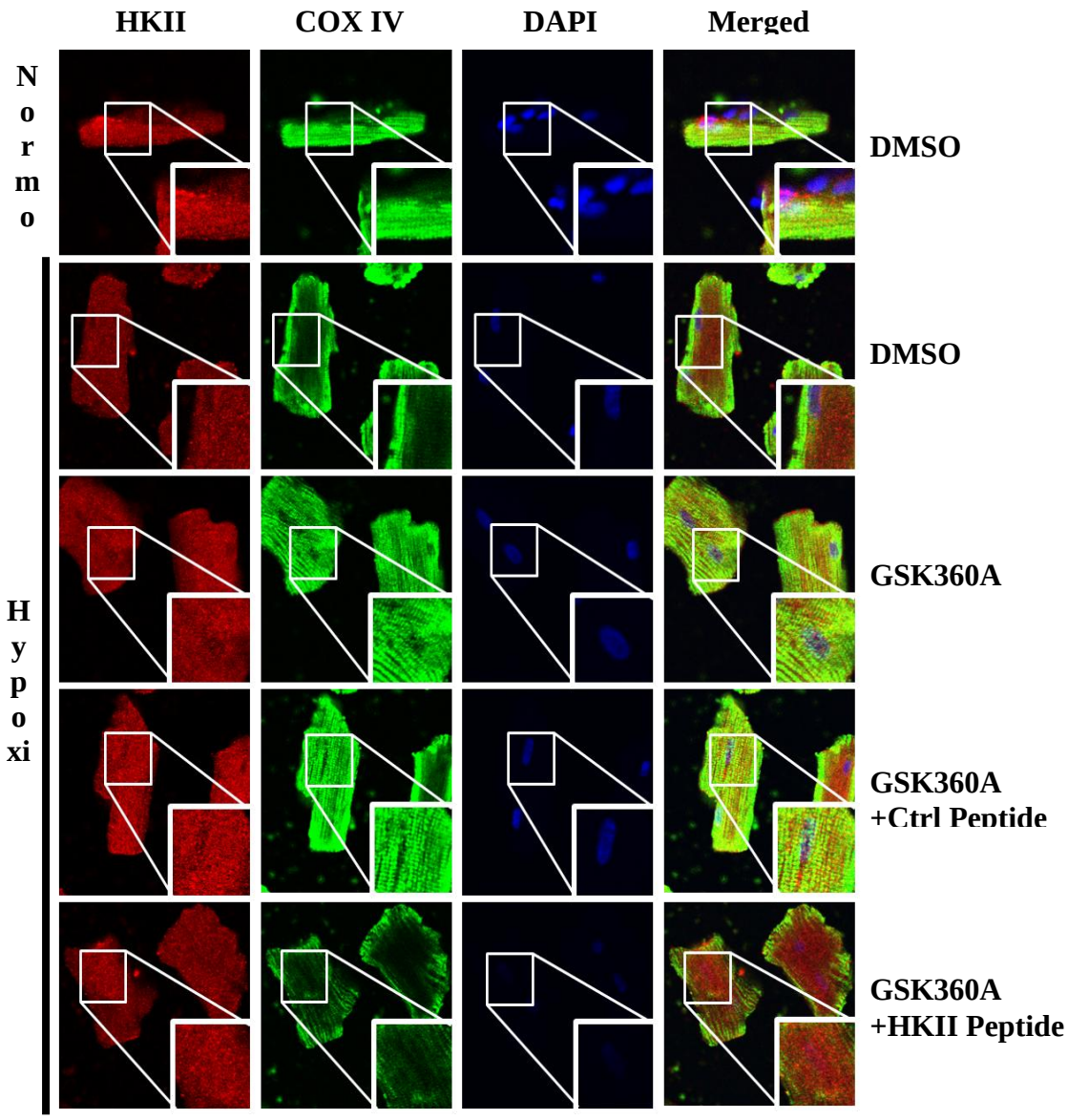

Figure S6. Confocal imaging of hexokinase II and COX IV in isolated adult rat cardiomyocytes following IRI.

REFERENCES

1. Smeele KM, Southworth R, Wu R, Xie C, Nederlof R, Warley A, Nelson JK, van Horssen P, van den Wijngaard JP, Heikkinen S, Laakso M, Koeman A, Siebes M, Eerbeek O, Akar FG, Ardehali H, Hollmann MW, Zuurbier CJ. Disruption of hexokinase II-mitochondrial binding blocks ischemic preconditioning and causes rapid cardiac necrosis. *Circ Res*. 2011;108:1165-1169
2. Di Lisa F, Menabo R, Canton M, Barile M, Bernardi P. Opening of the mitochondrial permeability transition pore causes depletion of mitochondrial and cytosolic nad+ and is a causative event in the death of myocytes in postischemic reperfusion of the heart. *J Biol Chem*. 2001;276:2571-2575